

· 专题研究 ·

# 内蒙古东乌珠穆沁旗早古生代辉长闪长岩年代学和地球化学特征及地质意义

杨泽黎, 王树庆, 胡晓佳, 辛后田, 李承东

(天津地质矿产研究所, 天津 300170)

**摘要:** 东乌旗乌拉盖地区出露一套早古生代辉长闪长岩, 为兴蒙造山带北缘二连-东乌旗早古生代岩浆岩带的组成部分。对该岩体进行了锆石 U-Pb 年龄、全岩地球化学及 Sr-Nd-Hf 同位素分析, 探讨了岩石成因及其对兴蒙造山带北缘早古生代构造演化的启示。锆石 LA-ICP-MS U-Pb 定年显示岩体年龄为  $499.6 \pm 1.2$  Ma, 为二连-东乌旗地区出露的最古老侵入体。岩体具有中等的  $\text{SiO}_2$  含量(51.60% ~ 54.28%), 富铝, 贫铁、镁, 全碱及钾含量较低, 属钙碱性岩浆系列; 富大离子亲石元素, 亏损高场强元素, 具有弱的 Eu 正异常( $\delta\text{Eu} = 1.03 \sim 1.34$ ), 稀土元素配分型式呈平缓的右倾型。辉长闪长岩同位素组成比较亏损, ( $^{87}\text{Sr}/^{86}\text{Sr}$ )<sub>i</sub> = 0.7045 ~ 0.7047,  $\varepsilon\text{Nd}(t) = +2.71 \sim +4.17$ ,  $\varepsilon\text{Hf}(t)$  相对  $\varepsilon\text{Nd}(t)$  明显偏高, 为 +10.8 ~ +18.7, 存在 Nd-Hf 同位素解耦现象。年代学、岩石地球化学以及 Sr-Nd-Hf 同位素综合分析表明, 乌拉盖辉长闪长岩是早古生代古亚洲洋沿苏左旗-锡林浩特一线向北俯冲的产物, 岩体形成于俯冲作用的初始阶段, 源区受到俯冲物质交代的地幔楔, 交代物质以板片熔体为主, 流体交代为辅, 无明显沉积物加入, 后期由于弧后拉张、贺根山洋盆打开与主体岛弧带脱离, 最终形成了与俯冲带彼此分隔的格局。

**关键词:** 辉长闪长岩; 早古生代; 兴蒙造山带; 古亚洲洋; 东乌珠穆沁旗

中图分类号: P588.12<sup>+2</sup>; P59

文献标识码: A

文章编号: 1000-6524(2018)03-0349-17

## Geochronology and geochemistry of Early Paleozoic gabbroic diorites in East Ujimqin Banner of Inner Mongolia and their geological significance

YANG Ze-li, WANG Shu-qing, HU Xiao-jia, XIN Hou-tian and LI Cheng-dong  
(Tianjin Institute of Geology and Mineral Resources, Tianjin 300170, China)

**Abstract:** The Wulagai early Paleozoic gabbroic diorite pluton is outcropped in the East Ujimqin Banner of Inner Mongolia. It is located on the northern margin of the Xing-Meng Orogenic Belt (XMOB) and was previously referred as part of the Erenhot-East Ujimqin Paleozoic magmatic belt. This study reports zircon U-Pb age, elemental and isotopic geochemical data of the pluton, so as to reveal its petrogenesis and implications for the evolution of the XMOB. Zircon U-Pb dating yielded a weighted mean age of  $499.6 \pm 1.2$  Ma, indicating that it is the earliest intrusive pluton in Erenhot-East Ujimqin Paleozoic magmatic belt. Geochemically, the Wulagai pluton shows moderate  $\text{SiO}_2$  (51.60% ~ 54.28%), high  $\text{Al}_2\text{O}_3$ , depletion of magnesium and iron, and low alkali and potassium, thus belonging to calc alkali rocks. The gabbroic diorites are also enriched in LILE, depleted in HFSE, and exhibit gradual right-oblique chondrite-normalized REE patterns with un conspicuous positive europium anomalies ( $\delta\text{Eu} = 1.03 \sim 1.34$ ). All the samples display depleted isotopic compositions with the data ( $^{87}\text{Sr}/^{86}\text{Sr}$ )<sub>i</sub> = 0.7045 ~ 0.7047

收稿日期: 2017-06-26; 接受日期: 2017-12-28

基金项目: 中国地质调查局地质矿产调查项目(DD20160041)

作者简介: 杨泽黎(1989- ), 男, 硕士, 助理工程师, 主要从事岩石学、地球化学研究及地质调查工作, E-mail: 812295251@qq.com。

and  $\varepsilon\text{Nd}(t) = +2.71 \sim +4.17$ , but the  $\varepsilon\text{Hf}(t)$  values of zircons ( $+10.8 \sim +18.7$ ) are much higher relative to the  $\varepsilon\text{Nd}(t)$  and show a Nd-Hf decoupling feature. Integrated geochemical, geochronological and Sr-Nd-Hf isotopic data suggest that the Wulagai gabbroic diorites were generated by the subduction of Paleo-Asian Ocean along the Sunid-Xilinhhot island arc in early Paleozoic, and were formed at the initial stage of the subduction. The rocks originated from a mantle wedge which was mainly modified by the slab-derived melt prior to fluids, and there were also indistinct sedimentary materials in the source. The back-arc extension and opening of Hegenshan Ocean possibly led to the separation of Wulagai pluton from the Sunid-Xilinhhot island arc. Along with the closure of Paleo-Asian Ocean, the pluton was ultimately isolated from the subduction zone by Hegenshan ophiolite complex.

**Key words:** gabbroic diorite; Early Paleozoic; Xing-Meng Orogenic Belt; Paleo-Asian Ocean; East Ujimqin Banner

**Fund support:** Project of China Geological Survey(DD20160041)

中亚造山带是世界上显生宙地壳增生与改造最为显著的地区(Jahn *et al.*, 2004; Hong *et al.*, 2004; Wang *et al.*, 2009),自新元古代亚洲洋裂解以来,中亚造山带经历了长期复杂的地质演化,在区域内形成了大面积分布的岩浆岩带,同时伴生了众多铜、金、稀土等多金属矿床(Badarch *et al.*, 2002; Khain *et al.*, 2003; Windley *et al.*, 2007; 肖文交等, 2008; Kröner *et al.*, 2014; Liu *et al.*, 2017),其地质演化历史一直是地学研究的热点。

作为中亚造山带东段重要组成部分,兴蒙造山带记录了古亚洲洋俯冲及西伯利亚和华北板块碰撞拼合的重要信息(Xiao *et al.*, 2003; Li, 2006; Jian *et al.*, 2008; Xu *et al.*, 2015; Song *et al.*, 2015),正确认识兴蒙造山带的地质演化对于恢复中亚造山带的构造历史有着重要的意义。

目前研究表明,古亚洲洋在早古生代经历了南北两侧的双向俯冲,分别在北部的苏尼特左旗-锡林浩特一线和南部的巴特敖包-白乃庙-温都尔庙-正镶白旗一线形成了两条岛弧岩浆岩带,前者包括苏左旗白音宝力道岛弧侵入岩(陈斌等,2001;石玉若等,2005;Jian *et al.*, 2008)、锡林浩特乌兰敖包图等岩体(王树庆等,2016),后者则以图古日格、巴特敖包和太古生庙岩体为代表(陶继雄等,2005;张维等,2008;白新会等,2015),并与同期的白乃庙群(Li *et al.*, 2015)、包尔汉图群火山岩伴生(尚恒胜等,2003)。除以上两条岩浆岩带外,在贺根山北侧二连-东乌旗地区也有部分早古生代岩浆岩存在,主要包括阿巴嘎旗北部的吉尔嘎郎图岩体,东乌旗马勒格

黑敖包、朝不楞以及乌拉盖等岩体,然而前人对该岩浆岩带及其地质构造背景研究相对较少,制约了对早古生代兴蒙造山带北缘构造演化历史的认识。本次选择东乌旗乌拉盖地区早古生代辉长闪长岩为对象,在锆石U-Pb年代学、岩石学和地球化学分析基础上,结合区域上同期岩浆作用的研究,探讨了岩石成因及源区性质,并通过对大地构造背景的讨论为这一地区早古生代构造演化提供相应约束。

## 1 地质背景及岩石学特征

乌拉盖地区位于东乌珠穆沁旗东部,大地构造位置属于西伯利亚板块南缘的乌里雅斯太活动陆缘(Xiao *et al.*, 2003, 图1a),二连-贺根山深断裂和乌努尔-鄂伦春断裂分别自研究区南部和北部通过。研究区外围大面积分布中生代的塔木兰沟组、玛尼吐组及满克头鄂博组等火山岩地层,北部则被晚古生代的宝力高庙组陆相火山-沉积岩系不整合覆盖(图1b)。此外,区域内还分布有少量奥陶系铜山组、多宝山组地层,前者散布于岩体周边,为一套半深海相碎屑沉积建造,后者则位于研究区北侧约10 km处,主要由中基性火山岩夹岩屑石英砂岩、泥岩组成(骆满生,2016)<sup>①</sup>,可能为岛弧火山作用的产物。

研究区侵入岩整体规模不大,但岩浆作用时代跨度较长,加里东期、海西期、燕山期岩体均有发育(图1b),其中早古生代岩浆岩主要包括石英闪长岩及辉长闪长岩两类,本次工作即对后者进行了取样

<sup>①</sup> 骆满生. 2016. 冬贵敖包等四幅1:50 000区域地质调查报告.

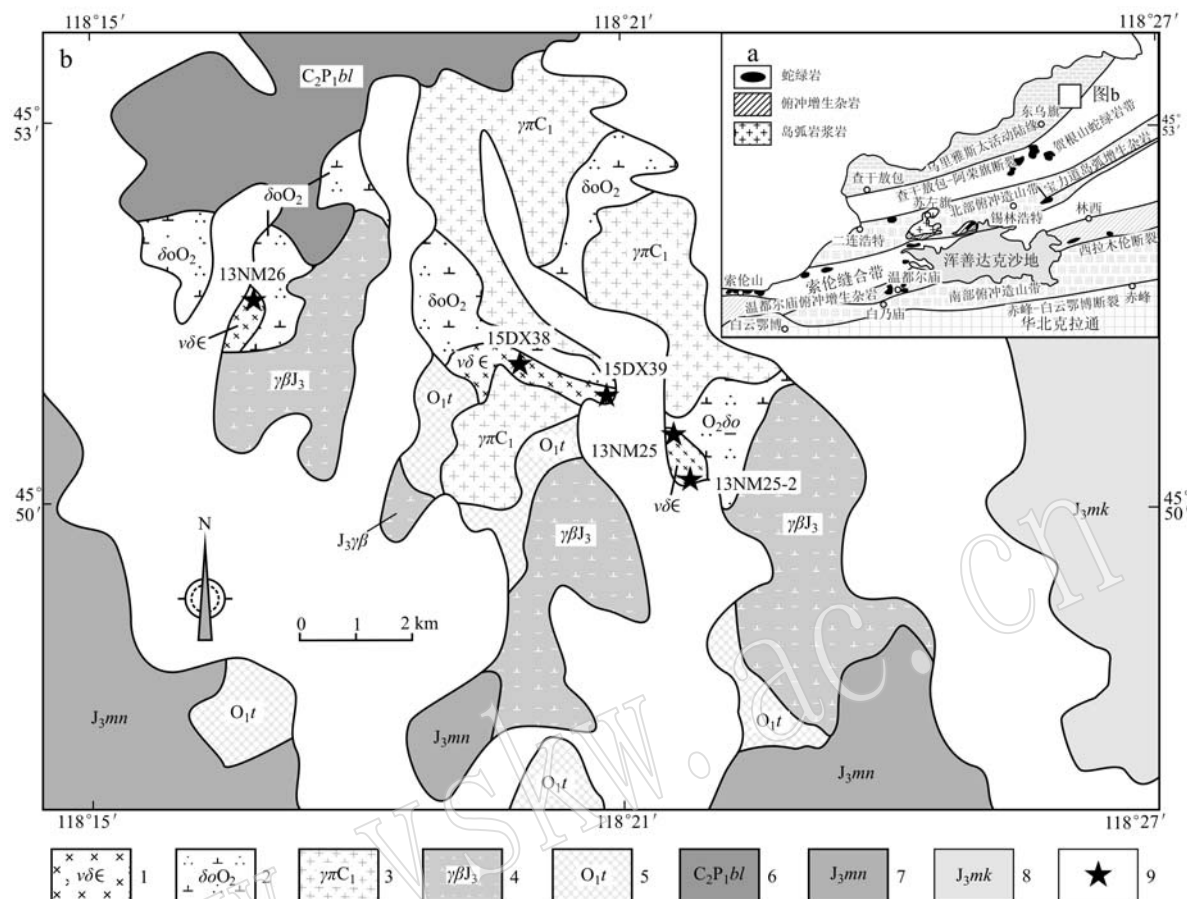


图 1 乌拉盖岩体构造位置(a, 据 Xiao et al., 2003; Li et al., 2014)及地质简图(b, 据骆满生, 2016)<sup>❶</sup>  
 Fig. 1 Maps showing tectonic location (a, after Xiao et al., 2003; Li et al., 2014) and geological sketch map (b, modified after Luo Mansheng, 2016)<sup>❶</sup> of the Wulagai gabbroic diorites

1—早古生代辉长闪长岩;2—早古生代石英闪长岩;3—晚古生代花岗斑岩;4—中生代黑云母花岗岩;5—铜山组;6—宝力高庙组;

7—玛尼吐组;8—满克头鄂博组;9—采样点

1—Early Paleozoic gabbroic diorites ; 2—Early Paleozoic quartz diorite ; 3—Late Paleozoic granite porphyry ; 4—Mesozoic biotite granite ;  
 5—Tongshan Formation ; 6—Baoligaomiao Formation ; 7—Manitu Formation ; 8—Mankoto Obo Formation ; 9—sampling site

研究。辉长闪长岩野外呈岩株或岩滴状产出,普遍被海西期及燕山期侵入体穿切改造,地表露头有限,整体出露面积约2~3 km<sup>2</sup>,并与南侧下奥陶统铜山组碎屑岩不整合接触。岩体内部未见脉体,露头尺度来看整体较为均匀,未见明显堆晶结构或岩相变化(图2a),矿物粒度2~4 mm,主要由基性斜长石、角闪石组成,辉石、石英及黑云母等含量较少,副矿物有锆石、磷灰石、磁铁矿和榍石等。主要矿物组分中,斜长石含量约为55%,半自形板条状,杂乱分布,聚片双晶非常发育,主要为拉长石,弱绢云母化、少量高岭土化;角闪石含量30%,半自形板条状或短柱

状,多色性Ng'=深黄绿,Np'=浅黄绿,次闪石化明显,部分角闪石颗粒内部及边缘嵌布板状斜长石;辉石含量较少,约10%,蚀变作用较强,核部偶见辉石残留;另有少量石英及黑云母呈填隙状分布各矿物之间(图2b)。

## 2 分析方法

### 2.1 锆石 U-Pb 定年及 Hf 同位素分析

将新鲜岩石样品破碎至80目,然后经水粗淘、强磁分选、电磁分选和酒精细淘之后,在显微镜下手

❶ 骆满生. 2016. 冬贵敖包等四幅1:50 000区域地质调查报告.

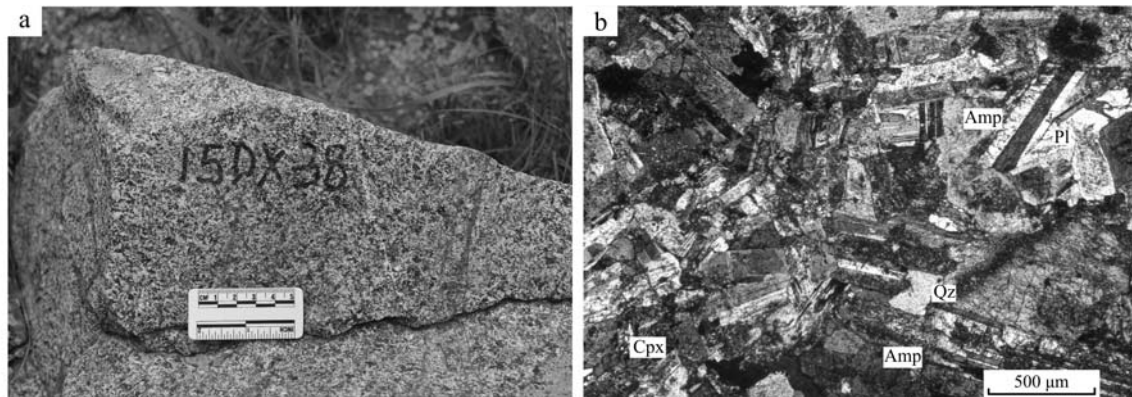


图2 乌拉盖辉长闪长岩野外及岩相学显微照片(+)

Fig. 2 Field outcrop and microphotographs (crossed nicols) of the Wulagai gabbroic diorites

Amp—角闪石; Pl—斜长石; Cpx—单斜辉石; Qz—石英  
Amp—amphibole; Pl—plagioclase; Cpx—clinopyroxene; Qz—quartz

工挑选出锆石,将待测锆石颗粒用环氧树脂制靶,然后磨至锆石颗粒的一半并抛光,并在北京锆年领航科技有限公司的日本电子JSM-6510型扫描电镜上进行阴极发光照相。锆石原位U-Pb年龄测试及原位Hf同位素测试均在天津地质矿产研究所同位素实验室利用激光剥蚀多接收器电感耦合等离子体质谱仪(LA-MC-ICPMS)完成,将NEW WAVE 193-FX-ArF准分子激光器与Thermo Fisher公司的Neptune多接收器电感耦合等离子体质谱仪联接,采用He气作为剥蚀物质载气。锆石U-Pb年龄测定使用的激光束斑直径为35 μm,剥蚀时间为30 s,采用美国国家标准技术研究院研制的人工合成硅酸盐标准参考物质NIST610,并利用澳大利亚锆石标样GEMOC/GJ-1( $^{207}\text{Pb}$ / $^{206}\text{Pb}$ 年龄为 $608.5 \pm 1.5$  Ma, Jackson *et al.*, 2004)作为内外标进行同位素分馏校正。对分析数据的离线处理(包括对样品和空白信号的选择、仪器灵敏度漂移校正、元素含量及U-Th-Pb同位素比值和年龄计算)均采用软件ICPMSDataCal 9.2 (Liu *et al.*, 2008, 2010a)完成,详细的仪器操作条件和数据处理方法见Liu等(2008, 2010a, 2010b)。U-Pb年龄谐和图绘制和年龄统计权重平均计算均采用Isoplot/Ex-ver3(Ludwig, 2003)完成。

锆石原位微区Hf同位素分析采用与U-Pb年龄测定相同的激光器与质谱仪,在锆石LA-ICP-MS U-Pb定年的基础上,参照锆石阴极发光(CL)图像,选择在原年龄测定点位置或附近进行。激光剥蚀束斑直径为50 μm,剥蚀时间为30 s,采用GJ-1作为外

标计算Hf同位素比值,具体仪器配置和实验流程参见耿建珍等(2011)。Hf同位素数据处理采用ICPMSDataCal 9.2程序完成(Liu *et al.*, 2010a)。

## 2.2 全岩元素及Sr-Nd同位素分析

全岩地球化学元素测试及Rb-Sr和Sm-Nd同位素组成分析均在天津地质矿产研究所实验室完成。野外采集新鲜无蚀变的岩石样品机械破碎至200目后送实验室分析。主量元素在样品制成熔片后通过X射线荧光光谱法(XRF)测试,X射线工作电压为50 kV,电流为50 mA,相对于标准样品的测定值,相对误差在元素丰度>1.0%时为±1%,元素丰度<1.0%时为±10%,FeO采用氢氟酸、硫酸溶样,重铬酸钾滴定容量法,分析精度优于2%,微量元素使用ICP-MS测试,样品测定值和推荐值的相对误差小于10%,且绝大多数值在5%以内。

Sr、Nd同位素比值测试均采用Triton热电离质谱进行测定,取200目全岩样品粉末(具体称样量以估计可取得1.0 μg以上的纯Nd为标准),用HF+HClO<sub>4</sub>+HNO<sub>3</sub>溶解,在密闭的Teflon溶样器中于高温条件下反应7 d。利用AG50W×12强酸性阳离子交换树脂分离Rb、Sr得到总稀土,然后采用HEHE-HP树脂(P507)技术分离纯化Nd,全流程空白本底稳定在Sm=3.0×10<sup>-11</sup> g, Nd=5.4×10<sup>-11</sup> g。Sr的质谱标准样NBS987 Sr的结果为<sup>87</sup>Sr/<sup>86</sup>Sr=0.710 245±30,LRIG质谱标准样的结果为<sup>143</sup>Nd/<sup>144</sup>Nd=0.512 202±30,国家一级标准Sm-Nd岩石样GBS04419的结果是:Sm=3.017×10<sup>-6</sup>,Nd=10.066×10<sup>-6</sup>,<sup>143</sup>Nd/<sup>144</sup>Nd=0.512 739±5。国际

标准岩石样BCR-2的结果是:  $\text{Rb} = (46.5 \pm 0.93) \times 10^{-6}$ ,  $\text{Sr} = (336.00 \pm 6.72) \times 10^{-6}$ ,  $^{87}\text{Sr}/^{86}\text{Sr} = 0.704\,958 \pm 30$ , Sr分馏的内校正因子采用 $^{88}\text{Sr}/^{86}\text{Sr} = 8.375\,209$ ,  $\text{Sm} = 6.70 \pm 0.14 \times 10^{-6}$ ,  $\text{Nd} = 28.00 \pm 0.56 \times 10^{-6}$ ,  $^{143}\text{Nd}/^{144}\text{Nd} = 0.512\,633 \pm 30$ 。Nd分馏的内校正因子采用 $^{146}\text{Nd}/^{144}\text{Nd} = 0.721\,9$ 。

### 3 分析结果

#### 3.1 锆石U-Pb年龄

本次研究对1件样品(13NM25)进行了锆石U-Pb定年,代表性锆石颗粒的阴极发光(CL)图像、测定点位及U-Pb年龄谐和图见图3。被测锆石多为无色或淡黄色,透明-半透明,多为棱柱状或短柱状,长

度100~200 μm,长宽比介于1~2。CL图像显示大部分锆石内部发育较宽的振荡环带,部分锆石还具有补片状或条带状均匀吸收(图3b),与中基性岩浆锆石特征吻合,被测锆石Th/U值均较高(0.20~0.55),为典型的岩浆结晶锆石(吴元保等,2004)。样品共获得24个测试点,在 $^{206}\text{Pb}/^{238}\text{U}-^{207}\text{Pb}/^{235}\text{U}$ 谐和图上均投影在谐和线上或谐和线附近(图3a), $^{206}\text{Pb}/^{238}\text{U}$ 表面年龄变化于503~493 Ma(表1),加权平均值为 $499.6 \pm 1.2$  Ma(MSWD=1.02, 2σ),为晚寒武世岩浆作用产物。这一年龄早于朝不楞辉长岩(461~450 Ma, 李红英等, 2016)、格日敖包二长花岗岩( $449 \pm 3$  Ma, 赵利刚等, 2012)以及吉尔嘎郎图花岗闪长岩(479~455 Ma, 作者未发表数据),为二连-东乌旗早古生代岩浆岩带内出露的最古老侵入体。

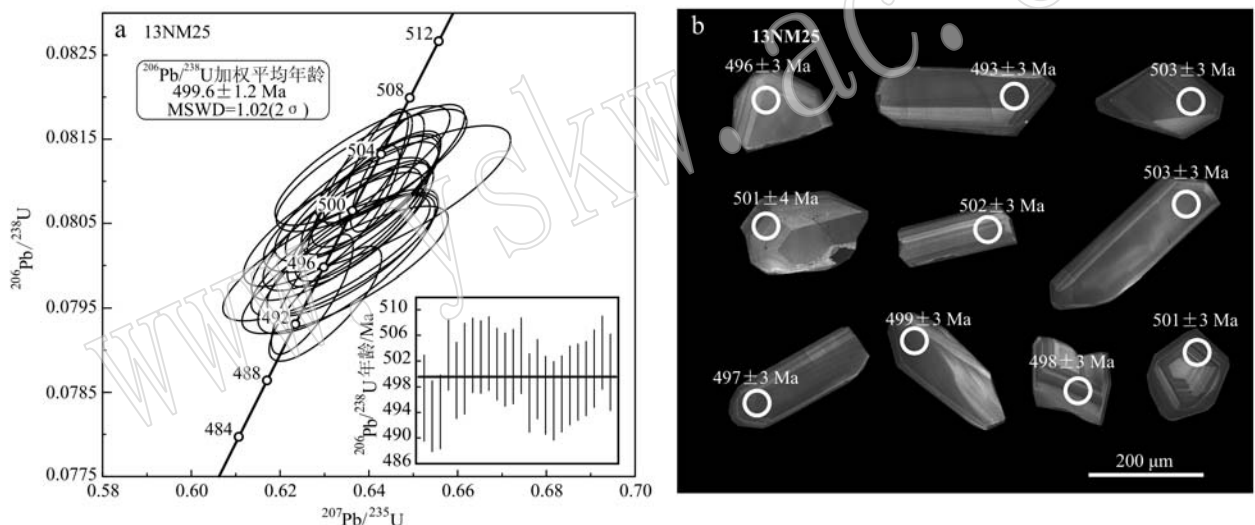


图3 乌拉盖辉长闪长岩被测锆石CL图像、LA-ICP-MS分析点位及U-Pb谐和图

Fig. 3 CL images, localities of the points for LA-ICP-MS measurements and the U-Pb concordia diagrams of zircons from the Wulagai gabbroic diorites

#### 3.2 主量元素

表2列出了乌拉盖辉长闪长岩的主微量元素分析结果及相关参数。从表中数据可以看出,样品均具有相似的地球化学特征,元素含量变化不大。岩体SiO<sub>2</sub>含量中等(51.60%~54.28%),铁镁钙含量偏低( $\text{Fe}_2\text{O}_3^T = 6.89\% \sim 9.86\%$ ,  $\text{MgO} = 5.67\% \sim 6.40\%$ ,  $\text{CaO} = 7.91\% \sim 9.85\%$ );全碱及钾含量不高,  $\text{K}_2\text{O} + \text{Na}_2\text{O}$ 变化于3.70%~5.15%之间, 碱度率指数(A. R.)为1.31~1.52,  $\text{K}_2\text{O}/\text{Na}_2\text{O} = 0.18 \sim 0.30$ , 在TAS关系图上落在亚碱性系列范围内(图4a),在  $\text{K}_2\text{O}-\text{SiO}_2$  图中被划分为钙碱性系列(图

4b)。辉长闪长岩在化学组成上的另一重要特征是富铝( $\text{Al}_2\text{O}_3 = 16.98\% \sim 18.06\%$ ),类似于岛弧和大陆边缘地区产出的高铝玄武岩,如印尼苏门答腊北部Barren低钾拉斑系列玄武岩  $\text{Al}_2\text{O}_3$  含量最高可达22.80% (Luhr and Haldar, 2006)。

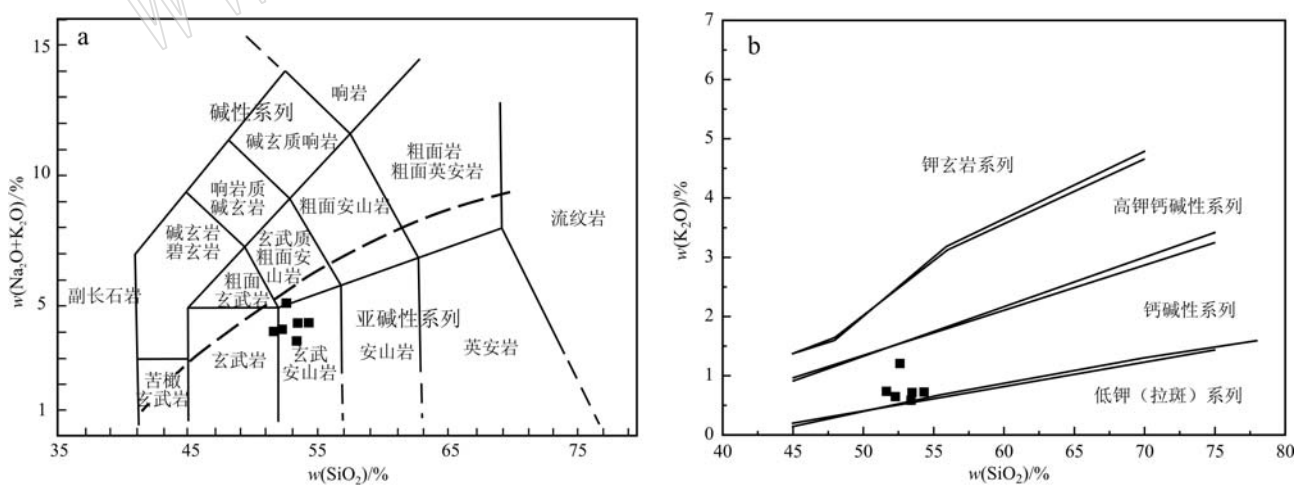
#### 3.3 微量及稀土元素

图5a为微量元素原始地幔标准化蛛网图,图5b为稀土元素球粒陨石标准化配分模式图。数据显示,乌拉盖辉长闪长岩富集Cs、Sr、Th、U等元素,Nb、Ta、Ti等高场强元素显著亏损,表现出消减带岩浆岩的典型特征(Condie, 1986),并与受俯冲板片

表1 乌拉盖辉长闪长岩 LA-ICP-MS 锆石 U-Pb 定年结果

Table 1 LA-ICP-MS zircon U-Pb dating results of the Wulagai gabbroic diorites

点号	同位素比值										年龄/Ma			
	$w_{\text{B}}/10^{-6}$	Th/U	$^{207}\text{Pb}/^{235}\text{U}$	$1\sigma$	$^{206}\text{Pb}/^{238}\text{U}$	$1\sigma$	$^{207}\text{Pb}/^{206}\text{Pb}$	$1\sigma$	$^{206}\text{Pb}/^{238}\text{U}$	$1\sigma$	$^{207}\text{Pb}/^{235}\text{U}$	$1\sigma$		
Pb	U													
样品 13NM25, 采样位置:E118°20'16", N45°51'15"														
13NM25-01	17	196	0.51	0.634 98	0.013 19	0.080 02	0.000 54	0.057 55	0.001 00	496	3	499	10	
13NM25-02	25	287	0.48	0.630 19	0.008 37	0.079 55	0.000 45	0.057 46	0.000 75	493	3	496	7	
13NM25-03	28	351	0.29	0.627 22	0.006 09	0.079 66	0.000 47	0.057 10	0.000 51	494	3	494	5	
13NM25-04	26	311	0.29	0.639 80	0.006 58	0.081 15	0.000 45	0.057 18	0.000 56	503	3	502	5	
13NM25-05	14	166	0.36	0.638 09	0.010 87	0.080 48	0.000 48	0.057 50	0.000 94	499	3	501	9	
13NM25-06	14	164	0.34	0.644 13	0.018 38	0.080 79	0.000 57	0.057 82	0.001 49	501	4	505	14	
13NM25-07	60	699	0.41	0.641 15	0.005 08	0.081 14	0.000 47	0.057 31	0.000 42	503	3	503	4	
13NM25-08	40	499	0.20	0.644 18	0.005 46	0.081 10	0.000 46	0.057 61	0.000 46	503	3	505	4	
13NM25-09	22	262	0.38	0.638 57	0.013 02	0.081 19	0.000 47	0.057 05	0.001 06	503	3	501	10	
13NM25-10	20	231	0.44	0.641 70	0.009 61	0.080 91	0.000 46	0.057 52	0.000 81	502	3	503	8	
13NM25-11	17	199	0.47	0.638 46	0.011 39	0.080 77	0.000 46	0.057 33	0.000 94	501	3	501	9	
13NM25-12	24	283	0.49	0.640 45	0.010 35	0.080 85	0.000 47	0.057 46	0.000 74	501	3	503	8	
13NM25-13	14	172	0.33	0.640 61	0.014 17	0.081 13	0.000 48	0.057 27	0.001 05	503	3	503	11	
13NM25-14	23	277	0.55	0.636 35	0.012 74	0.080 16	0.000 50	0.057 58	0.000 81	497	3	500	10	
13NM25-15	29	371	0.32	0.632 78	0.013 85	0.080 52	0.000 50	0.057 00	0.000 80	499	3	498	11	
13NM25-16	35	429	0.54	0.630 45	0.015 41	0.080 10	0.000 49	0.057 09	0.000 87	497	3	496	12	
13NM25-17	37	474	0.32	0.634 63	0.015 33	0.079 95	0.000 50	0.057 57	0.000 84	496	3	499	12	
13NM25-18	32	403	0.45	0.634 54	0.013 90	0.080 13	0.000 48	0.057 43	0.000 81	497	3	499	11	
13NM25-19	26	341	0.25	0.633 25	0.013 01	0.080 35	0.000 50	0.057 16	0.000 82	498	3	498	10	
13NM25-20	21	275	0.06	0.634 02	0.011 78	0.080 44	0.000 48	0.057 17	0.000 80	499	3	499	9	
13NM25-21	29	362	0.37	0.638 43	0.009 97	0.080 53	0.000 47	0.057 50	0.000 70	499	3	501	8	
13NM25-22	13	165	0.36	0.637 31	0.012 20	0.080 79	0.000 49	0.057 21	0.000 98	501	3	501	10	
13NM25-23	15	189	0.39	0.644 88	0.011 04	0.081 21	0.000 46	0.057 59	0.000 91	503	3	505	9	
13NM25-24	33	389	0.51	0.636 41	0.006 90	0.080 70	0.000 48	0.057 20	0.000 55	500	3	500	5	

图4 乌拉盖辉长闪长岩 ALK-SiO<sub>2</sub>(a, 底图据 Middlemost, 1994) 和 K<sub>2</sub>O-SiO<sub>2</sub>(b, 底图据 Le Maitre 等, 1989) 关系图Fig. 4 ALK-SiO<sub>2</sub>(a, after Middlemost, 1994) and K<sub>2</sub>O-SiO<sub>2</sub>(b, after Le Maitre et al., 1989) diagrams for the Wulagai gabbroic diorites

析出流体或熔体交代的地幔楔熔融形成的辉长质侵入岩十分相似(Wang et al., 2013), 暗示岩浆源区受

到了俯冲相关组分的影响。稀土元素组成上, 乌拉盖岩体稀土元素总量不高,  $\Sigma\text{REE}$ 为 $48.30 \times 10^{-6}$ ~

表 2 乌拉盖辉长闪长岩主量( $w_B/\%$ )、微量元素( $w_B/10^{-6}$ )组成及相关参数Table 2 Major ( $w_B/\%$ ), trace and rare earth element ( $w_B/10^{-6}$ ) content and related geochemical parameters of the Wulagai gabbroic diorites

样品号	13NM25	13NM25-2	13NM26	15DX38	15DX39	GS7594*	样品号	13NM25	13NM25-2	13NM26	15DX38	15DX39	GS7594*
SiO <sub>2</sub>	53.36	53.43	52.24	51.60	54.28	52.56	Pb	8.96	11.84	9.60	7.94	10.20	
TiO <sub>2</sub>	0.82	0.74	0.86	1.16	0.78	0.86	Zr	91.51	87.27	86.80	70.20	71.40	94.40
Al <sub>2</sub> O <sub>3</sub>	17.65	17.80	18.06	17.40	17.42	16.98	Hf	3.44	3.26	2.42	1.88	2.10	2.00
Fe <sub>2</sub> O <sub>3</sub> <sup>t</sup>	7.30	6.98	7.17	9.86	6.89	8.12	Y	17.41	17.09	16.30	14.90	15.40	19.00
MnO	0.13	0.13	0.13	0.14	0.12	0.16	Ba/Nb	46.43	45.49	48.05	59.64	48.69	33.06
MgO	5.95	5.67	6.03	6.28	5.82	6.40	Nb/U	8.04	5.69	6.04	3.38	4.94	4.15
CaO	9.85	9.14	9.56	8.25	8.84	7.91	La/Nb	2.31	2.52	2.69	3.59	3.07	1.69
Na <sub>2</sub> O	3.13	3.70	3.52	3.34	3.69	3.97	Th/Nb	0.74	0.91	0.91	1.01	1.00	0.89
K <sub>2</sub> O	0.57	0.70	0.63	0.72	0.71	1.19	Th/Yb	1.16	1.40	1.56	1.35	1.61	2.24
P <sub>2</sub> O <sub>5</sub>	0.09	0.09	0.08	0.10	0.09	0.13	La	7.29	7.56	8.28	8.01	8.20	9.10
LOI	1.60	2.05	0.96	1.15	1.45	1.69	Ce	15.85	16.05	18.00	23.70	17.40	19.20
ALK	3.70	4.39	4.15	4.06	4.40	5.16	Pr	2.11	2.12	2.51	2.14	2.44	2.86
K <sub>2</sub> O/Na <sub>2</sub> O	0.18	0.19	0.18	0.22	0.19	0.30	Nd	8.98	9.33	11.10	9.44	10.60	12.50
A. R.	1.31	1.39	1.35	1.38	1.40	1.52	Sm	2.15	2.23	2.78	2.41	2.63	2.95
Sc	30.39	31.02	20.40	26.80	20.50		Eu	0.97	0.94	0.95	0.85	0.90	1.06
V	180.2	189.9	218.0	428.0	206.0	148.3	Gd	2.29	2.34	2.86	2.60	2.66	3.13
Cr	37.03	38.47	40.10	31.00	37.00	46.00	Tb	0.46	0.45	0.46	0.45	0.45	0.57
Co	31.94	32.77	34.30	41.20	32.00	19.20	Dy	3.12	2.96	2.94	2.74	2.90	3.67
Ni	16.96	16.46	29.90	23.90	28.10	20.70	Ho	0.61	0.62	0.62	0.57	0.60	0.74
Cu	29.91	34.76	31.90	60.90	35.60	25.90	Er	1.88	1.83	1.75	1.57	1.64	2.19
Zn	70.49	77.12	95.50	70.70	81.60		Tm	0.31	0.31	0.27	0.24	0.24	0.36
Cs	1.31	2.00	1.12	1.43	1.60		Yb	2.01	1.95	1.80	1.67	1.65	2.14
Rb	12.27	19.39	14.60	20.00	19.50	26.70	Lu	0.27	0.28	0.28	0.25	0.25	0.34
Sr	333.2	406.5	336.0	342.0	364.0	349.0	$\Sigma$ REE	48.30	48.96	54.60	56.64	52.56	60.81
Ba	146.6	136.6	148.0	133.0	130.0	178.5	LR/HR	3.41	3.56	3.97	4.61	4.06	3.63
Th	2.33	2.72	2.80	2.25	2.66	4.80	(La/Yb) <sub>N</sub>	2.45	2.61	3.10	3.23	3.35	2.87
U	0.39	0.53	0.51	0.66	0.54	1.30	(La/Sm) <sub>N</sub>	2.14	2.13	1.87	2.09	1.96	1.94
Nb	3.16	3.00	3.08	2.23	2.67	5.40	(Gd/Yb) <sub>N</sub>	0.92	0.97	1.28	1.26	1.30	1.18
Ta	0.20	0.28	0.24	0.15	0.20	0.20	$\delta$ Eu	1.34	1.26	1.03	1.04	1.04	1.07

\* 样品数据引自骆满生(2016)①。

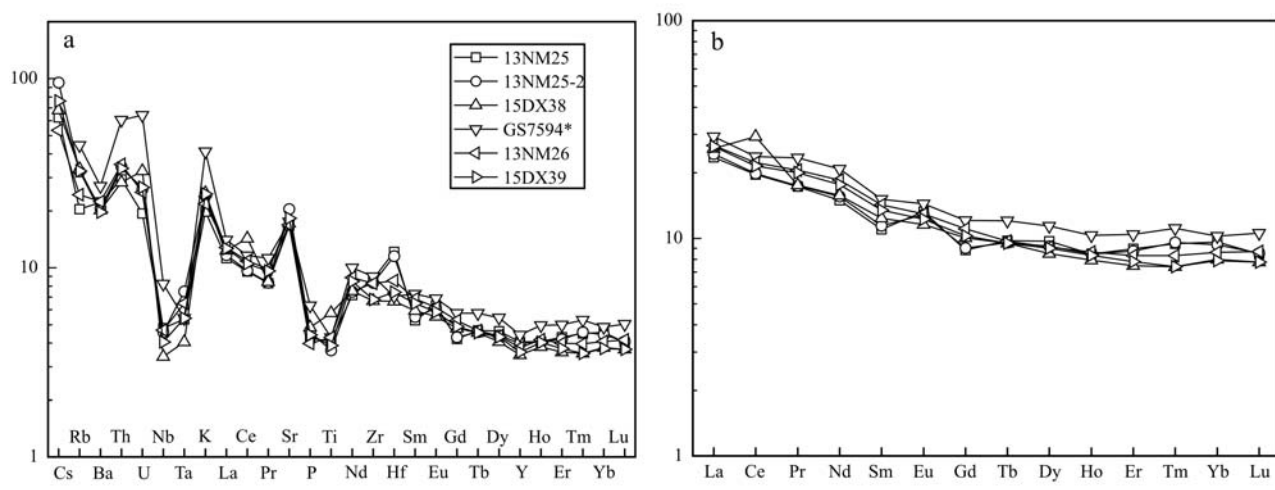


图 5 乌拉盖辉长闪长岩微量元素原始地幔标准化蛛网图(a)及稀土元素球粒陨石标准化配分曲线(b)

Fig. 5 Primitive mantle-normalized trace element spidergrams (a) and chondrite-normalized REE patterns (b) for the Wulagai gabbroic diorites

原始地幔标准化值据 McDonough 和 Sun (1995), 球粒陨石标准化值据 Boynton(1984)

the normalized values for primitive mantle after McDonough and Sun (1995), and for chondrite after Boynton (1984)

$60.81 \times 10^{-6}$ , 在球粒陨石标准化配分模式图中, 样品中等富集轻稀土元素, LREE/HREE 值为 3.41 ~ 4.61, 稀土元素配分型式呈平缓的右倾型, 轻重稀土元素分馏差异不大; 岩体无明显 Eu 负异常, 相反两件样品出现弱的 Eu 正异常 ( $\delta\text{Eu}$  值分别为 1.34、1.26), 结合岩体 Sr 较为富集, 说明岩体可能存在一定的斜长石的堆晶作用。

### 3.4 Sr-Nd-Hf 同位素

表 3 列出了乌拉盖岩体代表性样品的 Sr、Nd 同位素组成及根据年龄计算的有关参数。由表中数据可看出, 辉长闪长岩 ( $^{87}\text{Sr}/^{86}\text{Sr}$ )<sub>i</sub> = 0.703 5 ~ 0.704 7, ( $^{143}\text{Nd}/^{144}\text{Nd}$ )<sub>i</sub> = 0.512 133 ~ 0.512 207,  $\varepsilon\text{Nd}(t) = +2.71 \sim +4.17$ , 相应的 Nd 模式年龄  $t_{\text{DM}} = 1.09 \sim 1.27 \text{ Ga}$ , 在  $\varepsilon\text{Nd}(t) - (^{87}\text{Sr}/^{86}\text{Sr})_i$  图解(图 6a)中样品投影于 OIB 区域。与周边同时代火成岩相比, 乌拉盖岩体  $\varepsilon\text{Nd}(t)$  值近似于吉尔嘎郎图 (0.39 ~ 4.29, 作者未发表数据) 和白音宝力道 (-1.92 ~ 5.38, Jian et al., 2008) 岛弧岩浆岩, 略低于多宝山基性岛弧火山岩 (5.24 ~ 5.77, Wu et al.,

2015), 总体上具有相对亏损的同位素组成, 表明其主要来源于地幔物质的熔融。

此外, 本次研究在锆石 U-Pb 定年的基础上对样品进行了原位 Hf 同位素组成测定, 表 4 列出了测试结果及根据年龄计算的有关参数。由表中数据可看出, 所有测点的  $^{176}\text{Lu}/^{177}\text{Hf}$  值均小于 0.002, 说明锆石在形成后具有很少的放射性成因 Hf 的积累(吴福元等, 2007), 样品锆石的 ( $^{176}\text{Hf}/^{177}\text{Hf}$ )<sub>i</sub> 变化于 0.282 775 ~ 0.282 998 之间, 相应的  $\varepsilon\text{Hf}(t)$  值为 +10.8 ~ +18.7, 一阶段 Hf 模式年龄  $t_{\text{DM}}(\text{Hf})$  为 0.35 ~ 0.66 Ga(图 7a、7b)。整体来看样品  $\varepsilon\text{Hf}(t)$  值变化范围较小, 且同位素组成非常亏损, 在  $\varepsilon\text{Hf}(t) - t$  关系图上大部分样品点落在亏损地幔演化线附近, 部分样品甚至具有比原始地幔更加亏损的同位素组成(图 6b), 模式年龄也低于成岩年龄。这种极度亏损的特征一方面明确指示了岩浆来源于亏损地幔, 一方面也说明岩体可能发生了 Nd-Hf 同位素的解耦(吴福元等, 2007)。

表 3 乌拉盖辉长闪长岩 Sr-Nd 同位素组成

Table 3 Sr-Nd isotopic compositions of the Wulagai gabbroic diorites

样品	年龄/Ma	$^{87}\text{Rb}/^{86}\text{Sr}$	$^{87}\text{Sr}/^{86}\text{Sr}$	$I_{\text{Sr}}$	$^{147}\text{Sm}/^{144}\text{Nd}$	$^{143}\text{Nd}/^{144}\text{Nd}$	$I_{\text{Nd}}$	$\varepsilon\text{Nd}$	$t_{\text{DM}}/\text{Ga}$
13NM25	499.6	0.106 782	0.705 284	0.704 525	0.151 032	0.512 702	0.512 207	4.17	1.09
13NM25-2	499.6	0.138 056	0.705 676	0.704 693	0.150 943	0.512 627	0.512 133	2.71	1.27

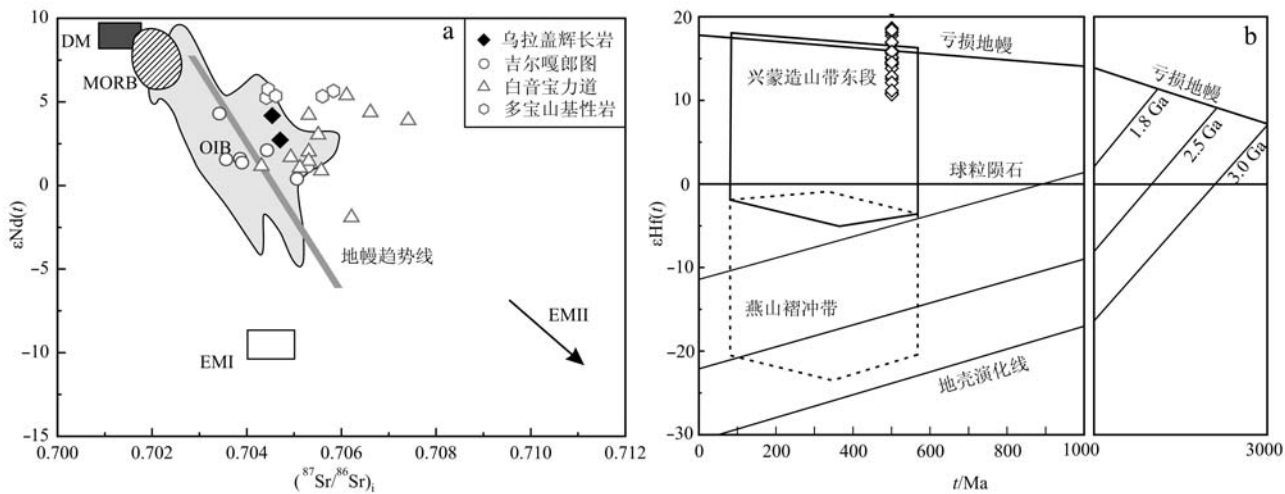


图 6 乌拉盖辉长闪长岩  $\varepsilon\text{Nd}(t) - (^{87}\text{Sr}/^{86}\text{Sr})_i$  关系图(a)和  $\varepsilon\text{Hf}(t) - t$  关系图(b)

Fig. 6  $\varepsilon\text{Nd}(t) - (^{87}\text{Sr}/^{86}\text{Sr})_i$  diagram (a) and  $\varepsilon\text{Hf}(t) - t$  plot (b) of the Wulagai gabbroic diorites

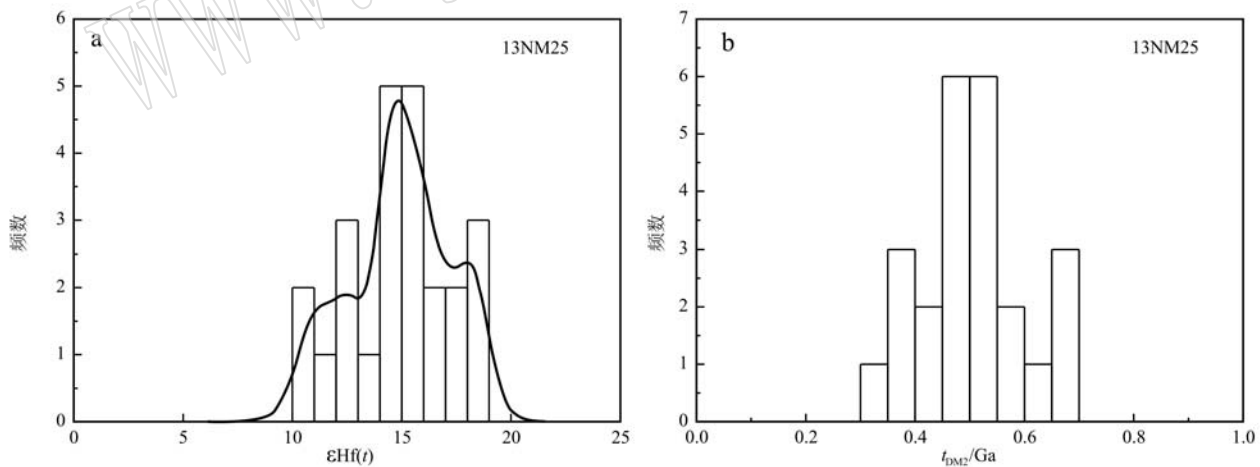
白音宝力道数据引自 Jian 等(2008)和作者未发表数据; 吉尔嘎郎图数据引自作者未发表数据; 多宝山数据引自 Wu 等(2015); 兴蒙造山带东段及燕山褶冲带引自 Yang 等(2006)、Xiao 等(2004)和 Chen 等(2009)

data of Baiyinbaolida after Jian et al. (2008) and the unpublished data of the authors; data of Jiergalangtu after the unpublished data of the authors; data of Duobaoshan after Wu et al. (2015); fields of East CAOB and YFTB after Yang et al. (2006), Xiao et al. (2004) and Chen et al. (2009)

表4 乌拉盖辉长闪长岩锆石 Hf 同位素分析结果

Table 4 Zircon Hf isotopic compositions of the Wulagai gabbroic diorites

点号	年龄/Ma	$^{176}\text{Yb}/^{177}\text{Hf}$	$^{176}\text{Lu}/^{177}\text{Hf}$	$^{176}\text{Hf}/^{177}\text{Hf}$	$2\sigma$	$(^{176}\text{Hf}/^{177}\text{Hf})_i$	$\varepsilon\text{Hf}(t)$	$2\sigma$	$t_{\text{DM}}/\text{Ma}$	$f_{\text{Lu/Hf}}$
样品:13NM25; 采样位置:E118°20'16", N45°51'15"										
1	499.6	0.019 622	0.000 559	0.283 003	0.000 021	0.282 998	18.7	0.7	348	-0.98
2	499.6	0.013 771	0.000 409	0.282 978	0.000 020	0.282 974	17.8	0.7	382	-0.99
3	499.6	0.046 142	0.001 274	0.282 893	0.000 024	0.282 881	14.5	0.8	513	-0.96
4	499.6	0.018 084	0.000 523	0.282 881	0.000 015	0.282 877	14.4	0.5	519	-0.98
5	499.6	0.013 470	0.000 467	0.282 889	0.000 018	0.282 885	14.7	0.6	507	-0.99
6	499.6	0.018 764	0.000 587	0.282 869	0.000 017	0.282 863	13.9	0.6	538	-0.98
7	499.6	0.055 955	0.001 939	0.282 845	0.000 019	0.282 827	12.6	0.7	592	-0.94
8	499.6	0.015 206	0.000 438	0.282 954	0.000 020	0.282 950	17.0	0.7	416	-0.99
9	499.6	0.010 624	0.000 339	0.282 987	0.000 017	0.282 984	18.2	0.6	369	-0.99
10	499.6	0.012 935	0.000 412	0.282 899	0.000 020	0.282 896	15.0	0.7	493	-0.99
11	499.6	0.054 933	0.001 593	0.282 928	0.000 027	0.282 913	15.7	0.9	467	-0.95
12	499.6	0.013 021	0.000 492	0.282 923	0.000 017	0.282 918	15.8	0.6	461	-0.99
13	499.6	0.007 608	0.000 222	0.282 994	0.000 020	0.282 992	18.4	0.7	359	-0.99
14	499.6	0.084 448	0.001 928	0.282 854	0.000 020	0.282 836	12.9	0.7	579	-0.94
15	499.6	0.036 582	0.001 036	0.282 824	0.000 022	0.282 814	12.2	0.8	608	-0.97
16	499.6	0.010 154	0.000 366	0.282 904	0.000 019	0.282 901	15.2	0.7	485	-0.99
17	499.6	0.012 599	0.000 434	0.282 928	0.000 016	0.282 924	16.0	0.6	453	-0.99
18	499.6	0.015 891	0.000 525	0.282 956	0.000 015	0.282 951	17.0	0.5	414	-0.98
19	499.6	0.012 800	0.000 515	0.282 924	0.000 017	0.282 919	15.9	0.6	459	-0.98
20	499.6	0.052 852	0.001 387	0.282 792	0.000 021	0.282 779	10.9	0.7	659	-0.96
21	499.6	0.040 988	0.001 269	0.282 787	0.000 027	0.282 775	10.8	0.9	665	-0.96
22	499.6	0.091 064	0.002 366	0.282 810	0.000 023	0.282 788	11.2	0.8	651	-0.93
23	499.6	0.039 047	0.001 130	0.282 894	0.000 019	0.282 883	14.6	0.7	510	-0.97
24	499.6	0.014 382	0.000 438	0.282 894	0.000 016	0.282 890	14.8	0.6	500	-0.99

图7 乌拉盖辉长闪长岩锆石  $\varepsilon\text{Hf}(t)$  值和二阶段 Hf 模式年龄( $t_{\text{DM}}$ )频数分布直方图Fig. 7 Histograms of zircon  $\varepsilon\text{Hf}(t)$  values and two-stage Hf model ages ( $t_{\text{DM}}$ ) for the Wulagai gabbroic diorites

## 4 讨论

### 4.1 岩体成因

Nb/U 值常作为判别地壳混染的指标(柴凤梅等, 2007), 乌拉盖岩体 Nb/U 值为 3.38 ~ 8.04, 低于

MORB 和 OIB ( $\text{Nb}/\text{U} = 47 \pm 10$ , Hofmann *et al.*, 1988), 也低于下地壳 ( $\text{Nb}/\text{U} \approx 25$ ; Rudnick and Gao, 2003) 和上地壳 ( $\text{Nb}/\text{U} \approx 9$ , Taylor and McLennan, 1985) 的平均值, 与通常遭受到地壳混染的玄武岩的 Nb/U 值明显不同(一般介于 9 ~ 40 之间, 葛文春等, 2001)。同时乌拉盖岩体锆石 Hf 同位素组成非常亏

损,这些特征暗示乌拉盖岩体没有经历明显的地壳混染作用,地球化学数据可以反映岩石成因及源区特征。如前所述,乌拉盖辉长闪长岩富集Cs、Rb、Sr等大离子亲石元素而亏损Nb、Ta、Ti等高场强元素,Th、U等不相容元素含量也较高,La/Nb、Ba/Nb值(分别为1.69~3.60和33.1~59.6)远高于亏损地幔起源的洋脊玄武岩(分别为1.07和4.30,Weaver, 1991),Nb/U、Ta/U值(分别为3.38~8.04和0.15~0.52)则明显偏低,这些特征与遭受俯冲交代作用的岛弧岩浆岩相似(Ayers, 1998);此外,在构造判别图解中(图8a、8b),所有样品均落于岛弧玄武岩或岛弧钙碱性玄武岩区域,在微量元素比值判别图解中(图8c、8d),样品则落在主动大陆边缘区域,

以上特征表明乌拉盖岩体应为活动大陆边缘环境下遭受俯冲交代的岛弧岩浆作用产物。事实上,现有研究表明,兴蒙造山带在早古生代经历了一系列大洋俯冲、地壳增生、多块体碰撞拼合、后造山伸展等构造事件,形成了数条俯冲增生型构造—岩浆岩带(Xiao et al., 2003; Xu et al., 2015),具体到乌拉盖地区,其北部蒙古境内存在多期次、多块体拼合的蒙古岛弧带(Badarach et al., 2002; Windley et al., 2007; Eizenhöfer et al., 2015),南部为古亚洲洋沿苏左旗—锡林浩特向北俯冲形成的岛弧岩浆岩带(Jian et al., 2008; Li et al., 2014; Xu et al., 2015, 图1a),因此,乌拉盖地区在早古生代应属于活跃的俯冲构造区域,而辉长闪长岩的地球化学特征则与早

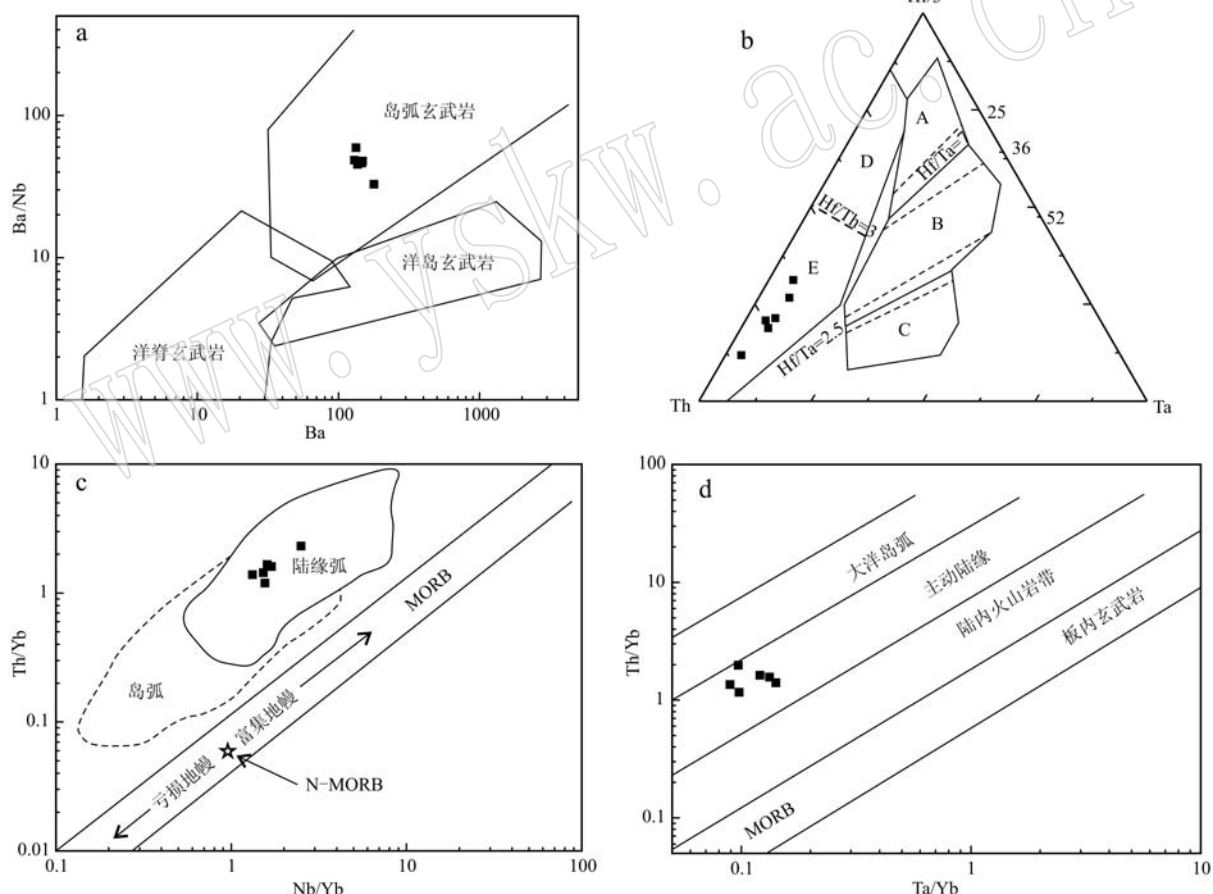


图8 乌拉盖辉长闪长岩构造判别图解

Fig. 8 Tectonic discrimination diagrams of the Wulagai gabbroic diorites

a—Ba/Nb-Ba图解(据Condie, 1989); b—Th-Ta-Hf图解(据Wood, 1980); c—Th/Yb-Nb/Yb图解(据Gorton and Schandl, 2000); d—Th/Yb-Ta/Yb图解(据Pearce and Peate, 1995); A—N-MORB; B—E-MORB及板内拉斑玄武岩; C—板内碱性玄武岩; D—岛弧拉斑玄武岩; E—岛弧钙碱性玄武岩

a—Ba/Nb-Ba diagram (after Condie, 1989); b—Th-Ta-Hf diagram (after Wood, 1980); c—Th/Yb-Nb/Yb diagram (after Gorton and Schandl, 2000); d—Th/Yb-Ta/Yb diagram (after Pearce and Peate, 1995); A—N-MORB; B—E-MORB and intraplate tholeiite; C—intraplate alkaline basalt; D—island arc tholeiite; E—island arc calc-alkali basalt

古生代构造背景吻合,是该时期陆缘岛弧岩浆作用的反映。

乌拉盖辉长闪长岩具有岛弧岩浆岩的地球化学特征,而岛弧基性岩特殊的地球化学特征通常被认为与俯冲物质对地幔楔的交代有关(Condie, 1986; 徐夕生等,2010)。对于俯冲交代物质,现有研究显示其可进一步区分为俯冲板片脱水产生的流体、板片熔融的熔体以及随俯冲板片进入地幔的沉积物等不同组分(Elliott *et al.*, 1997; Kelemen *et al.*, 2003; Hermann and Rubatto, 2009; Zamboni *et al.*, 2016),因而对岛弧岩浆源区组成还需进一步判别。俯冲板片流体和熔体在地球化学特征上常具有一定相似性,两者均可能导致岩浆中Nb、Ta等高场强元素的亏损(张海祥等,2005),不过两者微量元素分配系数仍有一定区别,比如高场强元素及重稀土元素在熔体中的含量较高,而碱金属、碱土金属、轻稀土元素则倾向于进入流体,故而可以通过不同种类元素比值的变化区分熔体及流体在交代作用中的贡献(Johnson and Plank, 1999; Turner *et al.*, 2003; Zamboni *et al.*, 2016):在Th/Nb—La/Nb以及Th/Nb—Ba/Nb判别图中(图9a、9b),乌拉盖岩体元素演化趋势与巽他岛弧近似,显示出熔体交代特征,与流体交代趋势明显不同,这表明俯冲物质对乌拉盖源区的交代应以熔体交代为主、流体交代为辅。另一方面,俯冲板片沉积物通常具有富集的同位素组成,少量沉积物混入即可明显改变岩浆的同位素特征(Straub *et al.*, 2015),而乌拉盖岩体 $\epsilon_{\text{Nd}}(t)=$

$+2.71 \sim +4.17$ ,  $\epsilon_{\text{Hf}}(t) = +10.8 \sim +18.7$ ,具有较为亏损的同位素组成,特别是Hf同位素,部分样品点 $\epsilon_{\text{Hf}}(t)$ 值甚至高于亏损地幔,因此,乌拉盖辉长闪长岩源区中应无明显沉积物组分加入。值得注意的是,Lu-Hf和Sm-Nd同位素体系通常具有正相关性( $\epsilon_{\text{Hf}} = 1.55 \epsilon_{\text{Nd}} + 1.21$ , Vervoort *et al.*, 2011),而乌拉盖岩体Hf同位素组成相对Nd明显偏高,出现了解耦现象。目前国内外对于Nd-Hf同位素解耦的原因仍存在争议,现有解释主要包括锆石效应(Vervoort *et al.*, 2000; Patchett *et al.*, 2004)、石榴子石效应(Patchett *et al.*, 2004; Schmitz *et al.*, 2004)和俯冲交代作用影响(Pearce *et al.*, 1999)等,然而锆石效应通常导致 $\epsilon_{\text{Hf}}$ 偏低,与乌拉盖岩体特征不符,另一方面,乌拉盖轻重稀土元素基本一致的分配型式也与源区存在石榴子石的假设冲突,因此,相对而言,乌拉盖岩体的同位素解耦更可能是受俯冲物质交代所致:在俯冲交代过程中,由于Nd比Hf更容易迁移,因而被交代作用改造的地幔楔将包含更多非放射成因Nd,即相对Nd来说源区放射成因Hf含量更高(Pearce *et al.*, 1999; Janney *et al.*, 2005)。这种解耦现象也从另一个侧面印证乌拉盖岩体的源区为经历了俯冲交代作用的地幔。

#### 4.2 地质意义

乌拉盖岩体为兴蒙造山带北部二连-东乌旗早古生代岩浆岩带的组成部分,目前对该岩浆岩带及其有关构造背景的研究相对较少,制约了对早古生代兴蒙造山带构造演化历史的认识。从前文讨论可

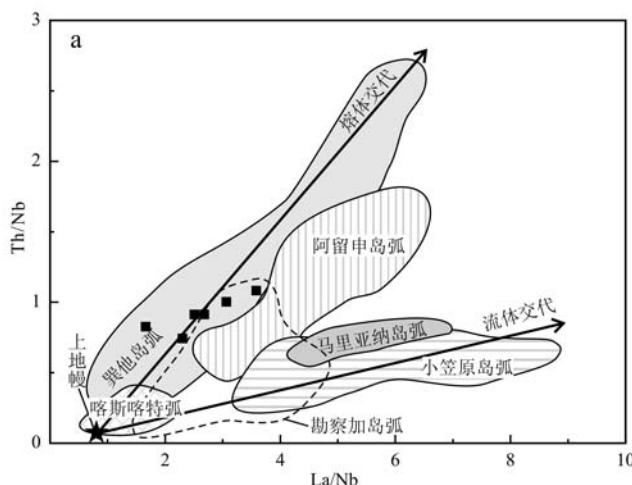
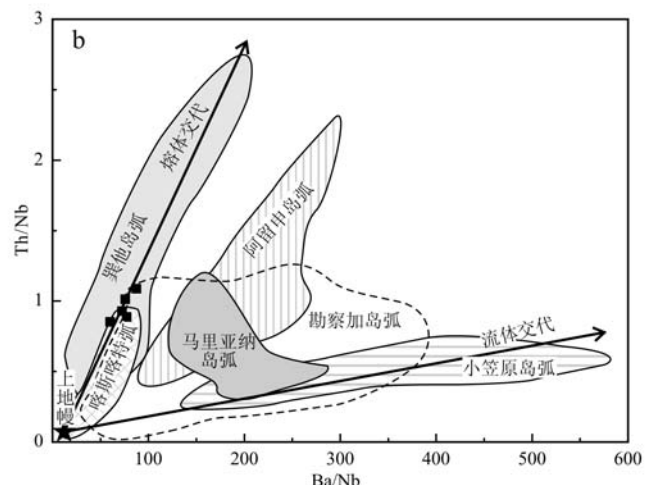


图9 乌拉盖辉长闪长岩板片熔体-流体交代判别图解(底图据Zamboni *et al.*, 2016)

Fig. 9 Element ratios discrimination diagrams between slab-derived fluid components and melt components of the Wulagai gabbroic diorites (base map after Zamboni *et al.*, 2016)



以看出,乌拉盖辉长闪长岩为岛弧环境下受俯冲交代作用影响的地幔楔熔融产物,同时,带内格日敖包、朝不楞等地的资料表明这些岩体也属于岛弧岩浆岩系列(赵利刚等,2012;李红英等,2016),再考虑到岩体北侧发育有同时期的多宝山组弧火山岩(杨文麟等,2014),因而二连-东乌旗地区在早古生代整体上应产出于俯冲岛弧环境。

然而虽然可以大致判定辉长闪长岩体的形成环境,但对于岩体所代表的岛弧岩浆岩带具体构造归属目前仍无明确结论。如前所述,岩浆岩带北侧在新元古代至早古生代期间经历了一系列俯冲-增生作用,在南蒙古地区形成了蒙古岛弧-岩浆岩带,岛弧带向西可延伸至蒙古西部,向东则与头道桥-嘎仙-新林蛇绿岩带相连,乌拉盖地区在构造位置上即属于蒙古岛弧南缘在中国境内的延伸(Badarch *et al.*, 2002; Windley *et al.*, 2007; Eizenhöfer *et al.*, 2015; Xiao *et al.*, 2015; Xu *et al.*, 2016),因此,如果仅从空间上来看,则岩体很有可能为新元古代-早古生代蒙古岛弧的产物。不过现有资料显示,与蒙古岛弧相关的蛇绿岩多形成于新元古代至寒武纪,如岛弧带西段 Bayankhongor 蛇绿岩形成时代为 654~535 Ma(Jian *et al.*, 2010), Khantaishi 蛇绿岩约为 568 Ma(Gibsher *et al.*, 2001), Banyannur 蛇绿岩约为 571 Ma(Khain *et al.*, 2003),岛弧带东段中国境内的头道桥蓝片岩形成时代为 516~511 Ma(Zhou *et al.*, 2015; Liu *et al.*, 2017),新林蛇绿岩为 539~510 Ma,嘎仙蛇绿岩约为 630 Ma(冯志强,2015),此外,葛文春(2005)、武广等(2005)在黑龙江北部识别出了年龄为 517~504 Ma 和 494~480 Ma 的后碰撞花岗岩,更限定了蒙古岛弧俯冲结束的时间。以上数据说明蒙古岛弧带的俯冲活动时间应主要集中于中寒武世之前,与之相对,乌拉盖辉长闪长岩形成于晚寒武世,加之近年来的地调工作在岩体周边识别出了数个形成时代介于 472.6~433.0 Ma 之间的岛弧花岗岩体(骆满生,2016<sup>①</sup>;田麒,2014<sup>②</sup>),并且岩浆岩带内其他岩体形成时代也都较晚,如朝不楞辉长岩形成年龄为 450~461 Ma(李红英等,2016),格日敖包岩体为 449 Ma(赵利刚等,2012)、吉尔嘎郎图岩体为 444.4~479.1 Ma(作者未发表数据),这些数据表明,乌拉盖辉长闪长岩与蒙古岛弧岩浆

作用并非一期,其可能仅代表了二连-东乌旗地区早古生代岛弧岩浆作用的开始,岩浆岩带整体活动高峰期应为中晚奥陶世,并持续至早志留世,明显晚于蒙古岛弧带的形成时间。综上所述,乌拉盖岩体的形成应与蒙古岛弧无关。

除北部的蒙古岛弧外,吉尔嘎郎图岩体南部苏左旗-锡林浩特-西乌旗一带还存在一条早古生代岛弧岩浆岩带,代表了古亚洲洋向北的俯冲碰撞(石玉若等,2005; Jian *et al.*, 2008; Li *et al.*, 2014; 王树庆,2016),岩浆岩带主要形成于 498~383 Ma 之间。其中 498~461 Ma 为洋陆俯冲阶段,伴随着岛弧岩浆作用和新生地壳的生成,440~434 Ma 为洋脊俯冲阶段,洋陆俯冲开始向弧陆碰撞转变,430~382 Ma 为陆块增生碰撞阶段,高钾花岗岩的侵位以及早泥盆世磨拉石的形成标志俯冲过程的结束并导致锡林浩特地区长英质岩体发生糜棱岩化(Jian *et al.*, 2008; Xu *et al.*, 2013; Li *et al.*, 2016, 2017a)。本文数据显示乌拉盖岩体形成年代为 499.6 Ma,其代表的岩浆岩带活动时间则可延续至晚奥陶-早志留世,从年代上看与苏左旗-西乌旗岛弧岩浆作用时期相近。另外,前人对区域上早古生代侵入岩体及多宝山弧火山岩的研究也倾向与该岛弧带有关,并认为这期岩浆岩与北侧的多宝山组岛弧火山岩构成了弧盆体系,为扎兰屯-多宝山弧后盆地的一部分(赵利刚等,2012; 王利民,2015; 李红英等,2016),而笔者通过对阿巴嘎旗北部空间上紧密相连的两个岩体——吉尔嘎郎图早中奥陶世岩体及格日敖包晚奥陶世岩体(作者未发表数据;赵利刚等,2012)的对比研究也发现,岩体特征大约在 445 Ma 发生了转变,岩性从 TTG 组合转变为 GG 组合,构造环境从火山弧转变为同碰撞环境,也与苏左旗-西乌旗地区洋陆俯冲向弧陆碰撞过渡的时间近似。综合以上分析,我们认为乌拉盖辉长闪长岩可能也为古亚洲洋在早古生代向北俯冲的产物,岩体形成于俯冲作用的开始阶段。不过在空间上,乌拉盖岩体与苏左旗-西乌旗岛弧带相隔较远,两者之间被晚古生代贺根山蛇绿岩带所分隔(图 1a)。现有研究认为贺根山洋为晚古生代板片拉张所产生的弧后盆地(Miao *et al.*, 2008; Eizenhöfer *et al.*, 2015; 黄波等,2016),因此,一个可能的模式为:乌拉盖岩体属于离俯冲带较远

<sup>①</sup> 骆满生. 2016. 冬贵敖包等四幅 1:50 000 区域地质调查报告.

<sup>②</sup> 田 麒. 2014. 查干楚鲁廷阿查等四幅 1:50 000 区域地质调查报告.

的岩浆弧或弧后盆地, 后期由于贺根山洋的打开与主体岛弧带分离, 最终在晚古生代随着贺根山洋的闭合, 形成了现今彼此分隔的格局。不过需要说明的是, 二连-东乌旗地区经历了多期大规模构造岩浆事件的改造, 同时目前对该区域的了解也不够深入, 以上所提出的仅为目前数据基础上获得的推论, 其中尚有一些不明确之处, 比如二连-东乌旗岩浆岩带与锡林浩特微陆块的关系, 虽然目前对锡林浩特微陆块的存在与否尚存争议(施光海等, 2003; 陈斌等, 2009; Li *et al.*, 2011; 孙立新等, 2013; Li *et al.*, 2017b), 但如果锡林浩特地区确实存在前寒武纪基底并与古亚洲洋发生了俯冲碰撞, 那显然二连-东乌旗早古生代岩体的形成机制将变得更加复杂, 甚至不排除有未识别的岛弧俯冲带存在的可能。诸如此类的问题都有待于将来更进一步的研究。

## 5 结论

(1) 锆石 U-Pb 定年结果表明, 乌拉盖辉长闪长岩形成时代为  $499.6 \pm 1.2$  Ma, 为二连-东乌旗早古生代岩浆岩带内出露的最古老侵入岩体。

(2) 地球化学及 Sr-Nd-Hf 同位素数据显示, 乌拉盖辉长闪长岩来源于岛弧环境下受到俯冲物质交代的地幔楔的部分熔融, 交代物质以板片熔体为主、流体交代为辅, 同时无明显大洋沉积物加入。

(3) 乌拉盖辉长闪长岩可能为早古生代古亚洲洋向北俯冲的产物, 岩体形成于俯冲作用的初始阶段, 它的侵位标志着二连-东乌旗早古生代岛弧岩浆作用的开始, 并一直持续至早志留世; 晚古生代由于弧后拉张、贺根山洋盆打开的影响, 二连-东乌旗岩浆岩带与主体岛弧带脱离, 最终形成了彼此分隔的格局。

## References

- Ayers J. 1998. Trace element modeling of aqueous fluid-peridotite interaction in the mantle wedge of subduction zones[J]. Contributions to Mineralogy and Petrology, 132: 390~404.
- Badarch G, Cunningham W D and Windley B F. 2002. A new terrane subdivision for Mongolia: Implications for the Phanerozoic crustal growth of Central Asia[J]. Journal of Asian Earth Sciences, 21(1): 87~110.
- Bai Xinhui, Xu Zhongyuan, Liu Zhenghong, *et al.* 2015. Zircon U-Pb dating, geochemistry and geological significance of the Early Silurian plutons from the southeastern margin of the Central Asian Orogenic Belt[J]. Acta Petrologica Sinica, 31(1): 67~79 (in Chinese with English abstract).
- Boynton W V. 1984. Geochemistry of the rare earth elements: meteorite studies[A]. Henderson P. Rare Earth Elements Geochemistry[C]. Amsterdam: Elsevier, 63~144.
- Chai Fengmei, Part A, Zhang Zhaochong, *et al.* 2007. Geochemistry of the lamprophyre dykes in the SW margin of the Tarim Block and their source region[J]. Geological Review, 53(1): 11~21 (in Chinese with English abstract).
- Chen B, Jahn B M and Tian W. 2009. Evolution of the Solonker suture zone: constraints from zircon U-Pb ages, Hf isotopic ratios and whole-rock Nd-Sr isotope compositions of subduction and collision-related magmas and forearc sediments[J]. J. Asian Earth Sci., 34: 245~257.
- Chen Bin, Ma Xinghua, Liu Ankun, *et al.* 2009. Zircon U-Pb ages of the Xilinhot metamorphic complex and blueschist, and implications for tectonic evolution of the Solonker suture[J]. Acta Petrologica Sinica, 25(12): 3123~3129 (in Chinese with English abstract).
- Chen Bin, Zhao Guochun and Wilde S. 2001. Subduction- and collision-related granitoids from Southern Sonidzuqi, Inner Mongolia: Isotopic ages and tectonic implications[J]. Geological Review, 47(4): 361~367 (in Chinese with English abstract).
- Condie K C. 1986. Geochemistry and tectonic setting of early Proterozoic supercrustal rocks in the south-western United States[J]. Journal of Geology, 94: 845~864.
- Condie K C. 1989. Geochemical changes in basalts and andesites across the Archaean-Proterozoic boundary: Identification and significance [J]. Lithos, 23: 1~18.
- Eizenhöfer P R, Zhao G, Sun M, *et al.* 2015. Geochronological and hfi isotopic variability of detrital zircons in paleozoic strata across the accretionary collision zone between the north China craton and Mongolian arcs and tectonic implications[J]. Geological Society of America Bulletin, 65(4): 487~508.
- Elliott T, Plank T, Zindler A, *et al.* 1997. Element transport from slab to volcanic front at the Mariana arc[J]. Journal of Geophysical Research Atmospheres, 102(B7): 14991~15020.
- Feng Zhiqiang. 2015. Paleozoic Tectonic-magmatic Evolution of Northern Great Hinggan Mountains[D]. Doctoral Dissertation: Jilin University, Changchun (in Chinese with English abstract).
- Ge Wenchun, Li Xianhua, Li Zhengxiang, *et al.* 2001. Mantle source and tectonic settings for the volcanic rocks from Danzhou group in

- Longsheng area, northern Guangxi[J]. Journal of Changchun University of Science and Technology, 31(1): 20~24(in Chinese with English abstract).
- Ge Wenchun, Wu Fuyuan, Zhou Changyong, et al. 2005. The age of Tahe granites of northern Greater Khingan Mountains and its constraints on the tectonic evolution of Erguana massif[J]. Chinese Science Bulletin, 50(12): 1 239~1 247(in Chinese).
- Geng Jianzhen, Li Huaikun, Zhang Jian, et al. 2011. Zircon Hf isotope analysis by means of LA-MC-ICP-MS[J]. Geological Bulletin of China, 30(10): 1 508~1 513(in Chinese with English abstract).
- Gibsher A S, Khain E V, Kotov A B, et al. 2001. Late Vendian age of the Han-Taishiri ophiolitic complex in western Mongolia[J]. Russ. Geol. Geophys., 42: 1 110~1 117.
- Gorton M P and Schandl E V. 2000. From Continents to Island Arcs: A Geochemical Index of Tectonic Setting for Arc-related and Within-plate Felsic to Intermediate Volcanic Rocks[J]. Canadian Mineralogist, 38(5): 1 065~1 073.
- Hermann J and Rubatto D. 2009. Accessory phase control on the trace element signature of sediment melts in subduction zones[J]. Chemical Geology, 265(3~4): 512~526.
- Hofmann A W. 1988. Chemical differentiation of the Earth: The relationship between mantle, continental crust, and oceanic crust[J]. Earth and Planetary Science Letters, 90: 297~314.
- Hong D W, Zhang J S, Wang T, et al. 2004. Continental crustal growth and the supercontinental cycle: Evidence from the Central Asian Orogenic Belt[J]. Journal of Asian Earth Science, 23: 799~813.
- Huang Bo, Fu Dong, Li Shuai, et al. 2016. The age and tectonic implications of the Hegenshan ophiolite in Inner Mongolia[J]. Acta Petrologica Sinica, 32(1): 158~176(in Chinese with English abstract).
- Jackson S E, Pearson N J, Griffin W L, et al. 2004. The application of laser ablation-inductively coupled plasma-mass spectrometry (LA-ICP-MS) to in situ U-Pb zircon geochronology[J]. Chemical Geology, 211: 47~69.
- Jahn B M, Capdevila R, Liu D Y, et al. 2004. Sources of Phanerozoic granitoids in the transect Bayanhongor-Ulaan Baatar, Mongolia: Geochemical and Nd isotopic evidence, and implications for Phanerozoic crustal growth[J]. Journal of Asian Earth Sciences, 23(5): 629~653.
- Janney P E, Roex A P L and Carlson R W. 2005. Hafnium isotope and trace element constraints on the nature of mantle heterogeneity beneath the central Southwest Indian ridge (13°E to 47°E)[J]. Journal of Petrology, 46(12): 1 137~1 141.
- Jian P, Kröner A, Windley B F, et al. 2010. Zircon ages of the Bayankhangor ophiolite mélange and associated rocks: Time constraints on Neoproterozoic to Cambrian accretionary and collisional orogenesis in central Mongolia[J]. Precambrian Research, 177(1): 162~180.
- Jian P, Liu D Y, Kröner A, et al. 2008. Time scale of the early to mid-Paleozoic orogenic cycle of the longlived Central Asian Orogenic Belt, Inner Mongolia of China: implications for continental growth[J]. Lithos, 101(3~4): 233~259.
- Johnson M C and Plank T. 1999. Dehydration and melting experiments constrain the fate of subducted sediments[J]. Geochemistry Geophysics Geosystems, 1(12): 583~597.
- Kelemen P B, Yogodzinski G M and Scholl D W. 2003. Along-strike variation in the Aleutian island arc: genesis of high Mg<sup>#</sup> andesite and implications for continental crust[J]. American Geophysical Union Geophysical Monograph, 138(1): 223~276.
- Khain E V, Bibikova E V, Salnikova E B, et al. 2003. The Palaeo-Asian Ocean in the Neoproterozoic and Early Palaeozoic: New geochronologic data and palaeotectonic reconstructions[J]. Precambrian Research, 122(1~4): 329~358.
- Kröner A, Kovach V, Belousova E, et al. 2014. Reassessment of continental growth during the accretionary history of the Central Asian Orogenic Belt[J]. Gondwana Research, 25(1): 103~125.
- Le Maitre R W, Bateman P, Dudek A, et al. 1989. A Classification of Igneous Rocks and Glossary of Terms[M]. Oxford: Blackwell.
- Li Hongying, Zhou Zhiguang, Li Pengju, et al. 2016. Geochemical features and significance of Late Ordovician gabbros in East Ujimqin Banner, Inner Mongolia[J]. Geological Review, 62(2): 300~316(in Chinese with English abstract).
- Li J Y. 2006. Permian geodynamic setting of Northeast China and adjacent regions: Closure of the Paleo-Asian Ocean and subduction of the paleo-Pacific Plate[J]. Journal of Asian Earth Sciences, 26(3~4): 207~224.
- Li W B, Hu C, Zhong R, et al. 2015. U-Pb, <sup>39</sup>Ar/<sup>40</sup>Ar geochronology of the metamorphosed volcanic rocks of the Bainaimiao Group in Central Inner Mongolia and its implications for ore genesis and geodynamic setting[J]. Journal of Asian Earth Sciences, 97: 251~259.
- Li Y L, Brouwer F M, Xiao W J, et al. 2016. Late Devonian to Early Carboniferous arc-related magmatism in the Baolidao arc, Inner Mongolia, China: Significance for southward accretion of the eastern Central Asian Orogenic Belt[J]. Geological Society of America Bulletin, 129(5~6): 677~697.
- Li Y L, Brouwer F M, Xiao W J, et al. 2017a. Subduction-related metasomatic mantle source in the eastern Central Asian Orogenic Belt: Evidence from amphibolites in the Xilingol Complex, Inner Mongolia,

- China[J]. *Gondwana Research*, 43: 193 ~ 212.
- Li Y L, Brouwer F M, Xiao W J, et al. 2017b. A Paleozoic fore-arc complex in the eastern Central Asian Orogenic Belt: Petrology, geochemistry and zircon U-Pb-Hf isotopic composition of paragneisses from the Xilingol Complex in Inner Mongolia, China[J]. *Gondwana Research*, 47: 323 ~ 341.
- Li Y L, Zhou H W, Brouwer F M, et al. 2011. Tectonic significance of the Xilin Gol Complex, Inner Mongolia, China: Petrological, geochemical and U-Pb zircon age constraints[J]. *Journal of Asian Earth Sciences*, 42(5): 1 018 ~ 1 029.
- Li Y L, Zhou H, Brouwer F M, et al. 2014. Early paleozoic to middle triassic bivergent accretion in the Central Asian Orogenic Belt: Insights from zircon U-Pb dating of ductile shear zones in central Inner Mongolia, China[J]. *Lithos*, 205(9): 84 ~ 111.
- Liu Y J, Li W M, Feng Z Q, et al. 2017. A review of the Paleozoic tectonics in the eastern part of Central Asian Orogenic Belt[J]. *Gondwana Research*, 43: 123 ~ 148.
- Liu Y S, Gao S, Hu Z C, et al. 2010a. Continental and oceanic crust recycling-induced melt-peridotite interactions in the Trans-North China Orogen: U-Pb dating, Hf isotopes and trace elements in zircons of mantle xenoliths[J]. *Journal of Petrology*, 51(1 ~ 2): 537 ~ 571.
- Liu Y S, Hu Z C, Gao S, et al. 2008. In situ analysis of major and trace elements of anhydrous minerals by LA-ICP-MS without applying an internal standard[J]. *Chemical Geology*, 257(1 ~ 2): 34 ~ 43.
- Liu Y S, Hu Z C, Zong K Q, et al. 2010b. Reappraisal and refinement of zircon U-Pb isotope and trace element analyses by LA-ICP-MS[J]. *Chinese Science Bulletin*, 55(15): 1 535 ~ 1 546.
- Ludwig K R. 2003. User's Manual for Isoplot 3.00: A Geochronological Toolkit for Microsoft Excel [M]. Berkeley Geochronology Center, Special Publication, 4: 1 ~ 71.
- Luhr J F and Haldar D. 2006. Barren Island Volcano (NE Indian Ocean): Island-arc high-alumina basalts produced by troctolite contamination[J]. *Journal of Volcanology and Geothermal Research*, 149(3 ~ 4): 177 ~ 212.
- McDonough W F and Sun S S. 1995. The composition of the Earth[J]. *Chemical Geology*, 120: 223 ~ 253.
- Miao L C, Fan W M, Liu D Y, et al. 2008. Geochronology and geochemistry of the Hegenshan ophiolitic complex: Implications for late-stage tectonic evolution of the Inner Mongolia-Daxinganling orogenic belt, China[J]. *Journal of Asian Earth Sciences*, 32(5 ~ 6): 348 ~ 370.
- Middlemost E A K. 1994. Naming materials in the magma/igneous rock system[J]. *Earth-Science Reviews*, 37(3 ~ 4): 215 ~ 224.
- Patchett P J, Vervoort J D, Söderlund U, et al. 2004. Lu-Hf and Sm-Nd isotopic systematics in chondrites and their constraints on the Lu-Hf properties of the Earth[J]. *Earth and Planetary Science Letters*, 222(1): 29 ~ 41.
- Pearce J A and Peate D W. 1995. Tectonic implications of the composition of volcanic arc magma[J]. *Annu. Rev. Earth Planet. Sci.*, 23: 251 ~ 285.
- Pearce J A, Kempton P D, Nowell G M, et al. 1999. Hf-Nd element and isotope perspective on the nature and provenance of mantle and subduction components in Western Pacific arc-basin systems[J]. *Journal of Petrology*, 40(11): 1 579 ~ 1 611.
- Rudnick R L and Gao S. 2003. Composition of the continental crust[A]. Holland H D and Turekian K K. *The Crust*[C]. Treatise on Geochemistry, 3. Elsevier-Pergamon, Oxford: 1 ~ 64.
- Schmitz M D, Vervoort J D, Bowring S A, et al. 2004. Decoupling of the Lu-Hf and Sm-Nd isotope systems during the evolution of granulitic lower crust beneath southern Africa[J]. *Geology*, 32(5): 405 ~ 408.
- Shang Hengsheng, Tao Jixiong, Baoyinwuliji, et al. 2003. The arc-basin system and tectonic significance of early Paleozoic in Baiyun' ebo Area Inner Mongolia[J]. *Geological Survey And Research*, 26(3): 160 ~ 168(in Chinese with English abstract).
- Shi Guanghai, Liu Dunyi, Zhang Fuqin, et al. 2003. SHRIMP U-Pb zircon dating of Xilin Gol Complex of Inner Mongolia, China, and its geological significances[J]. *Chinese Science Bulletin*, 48(20): 2 187 ~ 2 192(in Chinese).
- Shi Yuruo, Liu Dunyi, Zhang Qi, et al. 2005. The petrogenesis and SHRIMP dating of the Baiyinbaolidao adakitic rocks in southern Su-zuoqi, Inner Mongolia[J]. *Acta Petrologica Sinica*, 21(1): 143 ~ 150(in Chinese with English abstract).
- Song S G, Wang M M, Xu X, et al. 2015. Ophiolites in the Xing'an-Inner Mongolia accretionary belt of the CAOB: Implications for two cycles of seafloor spreading and accretionary orogenic events[J]. *Tectonics*, 34: 2 221 ~ 2 248.
- Straub S M, Gómez-Tuena A, Bindeman I N, et al. 2015. Crustal recycling by subduction erosion in the central Mexican Volcanic Belt[J]. *Geochimica et Cosmochimica Acta*, 166: 29 ~ 52.
- Sun Lixin, Ren Bangfang, Zhao Fengqing, et al. 2013. Zircon U-Pb dating and Hf isotopic compositions of the Mesoproterozoic granitic gneiss in Xilinhot Block, Inner Mongolia[J]. *Geological Bulletin of China*, 32(2): 327 ~ 340(in Chinese with English abstract).
- Tao Jixiong, Xu Liquan, He Feng, et al. 2005. Petrological evidence for subduction of the Early Paleozoic oceanic crust in Bart-Obo, Inner Mongolia[J]. *Geological Survey and Research*, 28(1): 1 ~ 8(in Chinese with English abstract).

- Chinese with English abstract).
- Taylor S R and McLennan S M. 1985. The Continental Crust: Its Composition and Evolution [M]. Oxford: Blackwell, 1~312.
- Turner S, Bourdon B and Gill J. 2003. Insights into magma genesis at convergent margins from U-series isotopes [J]. *Rev. Mineral. Geochim.*, 52(1): 255~315.
- Vervoort J D, Patchett P J, Albarède F, et al. 2000. Hf-Nd isotopic evolution of the lower crust [J]. *Earth and Planetary Science Letters*, 181: 115~129.
- Vervoort J D, Plank T and Prytulak J. 2011. The Hf-Nd isotopic composition of marine sediments [J]. *Geochimica et Cosmochimica Acta*, 75: 5 903~5 926.
- Wang Limin. 2015. Geochemistry of the Ordovician Volcanic Rocks in Aershan, Inner Mongolia and Its Tectonic Significance (Master Dissertation) [D]. Changchun: Jilin University (in Chinese with English abstract).
- Wang Shuqing, Xin Houtian, Hu Xiaojia, et al. 2016. Geochronology, geochemistry and geological significance of Early Paleozoic Wulanaobatu intrusive rocks, Inner Mongolia [J]. *Earth Science—Journal of China University of Geosciences*, 41(4): 555~569 (in Chinese with English abstract).
- Wang T, Jahn B M, Kovach P V, et al. 2009. Nd-Sr isotopic mapping of the Chinese Altai and implications for continental growth in the Central Asian Orogenic Belt [J]. *Lithos*, 110(1~4): 359~372.
- Wang Y J, Zhang A M, Fan W M, et al. 2013. Origin of paleo-subduction-modified mantle for Silurian gabbro in the Cathaysia Block: Geochronological and geochemical evidence [J]. *Lithos*, 160~161: 37~54.
- Weaver B L. 1991. The origin of ocean island basalt end-member compositions: Trace element and isotopic constraints [J]. *Earth and Planetary Science Letters*, 104(2~4): 381~397.
- Windley B F, Alexeiev D, Xiao W J, et al. 2007. Tectonic models for accretion of the Central Asian Orogenic Belt [J]. *Journal of the Geological Society*, 164: 31~47.
- Wood D A. 1980. The application of a Th-Hf-Ta diagram to problems of tectonomagmatic classification and to establishing the nature of crustal contamination of basaltic lavas of the British Tertiary volcanic province [J]. *Earth and Planetary Science Letters*, 50(1): 11~30.
- Wu F Y, Li X H, Zheng Y F, et al. 2007. Lu-Hf isotopic systematics and their application in petrology [J]. *Acta Petrologica Sinica*, 23(2): 185~220.
- Wu G, Chen Y, Sun F, et al. 2015. Geochronology, geochemistry, and Sr-Nd-Hf isotopes of the early paleozoic igneous rocks in the Duobaoshan area, NE China, and their geological significance [J]. *Journal of Asian Earth Sciences*, 97: 229~250.
- Wu Guang, Sun Fengyue, Zhao Caisheng, et al. 2005. Discovery of early Paleozoic post-collision granites in the northern Ergun Massif and its geological significance [J]. *Chinese Science Bulletin*, 50(20): 2 278~2 288 (in Chinese).
- Wu Yuanbao and Zheng Yongfei. 2004. Genesis of zircon and its constraints on interpretation of U-Pb age [J]. *Chinese Science Bulletin*, 49(15): 1 554~1 569 (in Chinese).
- Xiao Wenjiao, Shu Liangshu, Gao Jun, et al. 2008. Continental dynamics of the Central Asian Orogenic Belt and its metallogeny [J]. *Xinjiang Geology*, 26(1): 4~8 (in Chinese with English abstract).
- Xiao W J, Windley B F, Hao J, et al. 2003. Accretion leading to collision and the Permian Solonker Suture, Inner Mongolia, China: Termination of the Central Asian Orogenic Belt [J]. *Tectonics*, 22(6): 1 069~1 090.
- Xiao W J, Windley B, Sun S, et al. 2015. A tale of amalgamation of three collage systems in the Permian-Middle Triassic in Central Asia: Oroclines, sutures and terminal accretion [J]. *Annual Review of Earth and Planetary Sciences*, 43: 477~507.
- Xiao W J, Zhang L C, Qin K Z, et al. 2004. Paleozoic accretionary and collisional tectonics of the eastern Tianshan (China): Implications for the continental growth of Central Asia [J]. *Am. J. Sci.*, 304: 370~395.
- Xu B, Charvet J, Chen Y, et al. 2013. Middle Paleozoic convergent orogenic belts in western Inner Mongolia (China): Framework, kinematics, geochronology and implications for tectonic evolution of the Central Asian Orogenic Belt [J]. *Gondwana Research*, 23: 1 342~1 364.
- Xu B, Zhao G C, Li J H, et al. 2016. Ages and Hf isotopes of detrital zircons from Paleozoic strata in the Chagan Obo Temple area, Inner Mongolia: Implications for the evolution of the Central Asian Orogenic Belt [J]. *Gondwana Research*, 43: 149~163.
- Xu B, Zhao P, Wang Y Y, et al. 2015. The pre-Devonian tectonic framework of Xing'an-Mongolia Orogenic Belt (XMOB) in North China [J]. *Journal of Asian Earth Sciences*, 97(Part B): 183~196.
- Xu Xisheng and Qiu Jiansheng. 2010. Igneous Petrology [M]. Beijing: Science Press, 1~346 (in Chinese).
- Yang J H, Wu F Y, Shao J A, et al. 2006. Constraints on the timing of uplift of the Yanshan fold and thrust belt, North China [J]. *Earth and Planetary Science Letters*, 246(3~4): 336~352.
- Yang Wenlin, Luo Mansheng, Wang Chenggang, et al. 2014. Neoproterozoic-paleozoic sedimentary basins evolution of Xing-Meng Orogenic Belt [J]. *Earth Science-Journal of China University of Geosciences*, 39(8): 1 155~1 168 (in Chinese with English abstract).

- Zamboni D, Gazel E, Ryan J, et al. 2016. Contrasting sediment melt and fluid signatures for magma components in the Aeolian arc: Implications for numerical modeling of subduction systems[J]. *Geochemistry Geophysics Geosystems*, 17(6): 2 034 ~ 2 053.
- Zhang Haixiang, Zhang Boyou and Niu Hecai. 2005. Nb-enriched basalt: the product of the partial melting of the slab-derived melt metasomatized mantle peridotite[J]. *Advances in Earth Science*, 20(11): 1 234 ~ 1 242 (in Chinese with English abstract).
- Zhang Wei and Jian Ping. 2008. SHRIMP dating of Early Paleozoic granites from North Damaoqi, Inner Mongolia[J]. *Acta Geologica Sinica*, 82(6): 778 ~ 787 (in Chinese with English abstract).
- Zhao Ligang, Ran Hao, Zhang Qinghong, et al. 2012. Discovery of Ordovician pluton in Abaga Banner, Inner Mongolia and its geological significance[J]. *Global Geology*, 31(3): 451 ~ 461 (in Chinese with English abstract).
- Zhou J B, Wang , Wilde S A, et al. 2015. Geochemistry and U-Pb zircon dating of the Toudaoqiao blueschists in the great Xing'an range, northeast China, and tectonic implications [J]. *Journal of Asian Earth Sciences*, 97: 197 ~ 210.

## 附中文参考文献

- 白新会, 徐仲元, 刘正宏, 等. 2015. 中亚造山带东段南缘早志留世岩体锆石U-Pb定年、地球化学特征及其地质意义[J]. *岩石学报*, 31(1): 67 ~ 79.
- 柴凤梅, 帕拉提·阿布都卡迪尔, 张招崇, 等. 2007. 塔里木板块西南缘钾质煌斑岩地球化学及源区特征[J]. *地质论评*, 53(1): 11 ~ 21.
- 陈斌, 马星华, 刘安坤, 等. 2009. 锡林浩特杂岩和蓝片岩的锆石U-Pb年代学及其对索伦缝合带演化的意义[J]. *岩石学报*, 25(12): 3 123 ~ 3 129.
- 陈斌, 赵国春, Wilde S. 2001. 内蒙古苏尼特左旗南两类花岗岩同位素年代学及其构造意义[J]. *地质论评*, 47(4): 361 ~ 367.
- 冯志强. 2015. 大兴安岭北段古生代构造-岩浆演化(博士学位论文) [D]. 长春: 吉林大学.
- 葛文春, 李献华, 李正祥, 等. 2001. 桂北龙胜丹洲群火山岩的地幔源区及大地构造环境[J]. *长春科技大学学报*, 31(1): 20 ~ 24.
- 葛文春, 吴福元, 周长勇, 等. 2005. 大兴安岭北部塔河花岗岩的时代及对额尔古纳地块构造归属的制约[J]. *科学通报*, 50(12): 1 239 ~ 1 247.
- 耿建珍, 李怀坤, 张健, 等. 2011. 锆石Hf同位素组成的LA-MC-ICP-MS测定[J]. *地质通报*, 30(10): 1 508 ~ 1 513.
- 黄波, 付冬, 李树才, 等. 2016. 内蒙古贺根山蛇绿岩形成时代及构造启示[J]. *岩石学报*, 32(1): 158 ~ 176.
- 李红英, 周志广, 李鹏举, 等. 2016. 内蒙古东乌珠穆沁旗晚奥陶世辉长闪长岩地球化学特征及其地质意义[J]. *地质论评*, 62(2): 300 ~ 316.
- 尚恒胜, 陶继雄, 宝音乌力吉, 等. 2003. 内蒙古白云鄂博地区早古生代弧-盆体系及其构造意义[J]. *地质调查与研究*, 26(3): 160 ~ 168.
- 施光海, 刘敦一, 张福勤, 等. 2003. 中国内蒙古锡林郭勒杂岩SHRIMP锆石U-Pb年代学及意义[J]. *科学通报*, 48(20): 2 187 ~ 2 192.
- 石玉若, 刘敦一, 张旗, 等. 2005. 内蒙古苏左旗白音宝力道Adakite质岩类成因探讨及其SHRIMP年代学研究[J]. *岩石学报*, 21(1): 143 ~ 150.
- 孙立新, 任邦方, 赵凤清, 等. 2013. 内蒙古锡林浩特地块中元古代花岗片麻岩的锆石U-Pb年龄和Hf同位素特征[J]. *地质通报*, 32(2): 327 ~ 340.
- 陶继雄, 许立权, 贺锋, 等. 2005. 内蒙古巴特敖包地区早古生代洋壳消减的岩石证据[J]. *地质调查与研究*, 28(1): 1 ~ 8.
- 王利民. 2015. 内蒙古阿尔山地区奥陶纪火山岩地球化学特征及其构造意义(硕士学位论文)[D]. 长春: 吉林大学.
- 王树庆, 辛后田, 胡晓佳, 等. 2016. 内蒙古乌兰敖包图早古生代侵入岩年代学、地球化学特征及地质意义[J]. *地球科学——中国地质大学学报*, 41(4): 555 ~ 569.
- 吴福元, 李献华, 郑永飞, 等. 2007. Lu-Hf同位素体系及其岩石学应用[J]. *岩石学报*, 23(2): 185 ~ 220.
- 吴元保, 郑永飞. 2004. 锆石成因矿物学研究及其对U-Pb年龄解释的制约[J]. *科学通报*, 49(16): 1 589 ~ 1 604.
- 武广, 孙丰月, 赵财胜, 等. 2005. 额尔古纳地块北缘早古生代后碰撞花岗岩的发现及其地质意义[J]. *科学通报*, 50(20): 2 278 ~ 2 288.
- 肖文交, 舒良树, 高俊, 等. 2008. 中亚造山带大陆动力学过程与成矿作用[J]. *新疆地质*, 26(1): 4 ~ 8.
- 徐夕生, 邱检生. 2010. 火成岩石学[M]. 北京: 科学出版社, 1 ~ 346.
- 杨文麟, 骆满生, 王成刚, 等. 2014. 兴蒙造山系新元古代-古生代沉积盆地演化[J]. *地球科学——中国地质大学学报*, 39(8): 1 155 ~ 1 168.
- 张海祥, 张伯友, 牛贺才. 2005. 富铌玄武岩: 板片熔体交代的地幔橄榄岩部分熔融产物[J]. *地球科学进展*, 20(11): 1 234 ~ 1 242.
- 张维, 简平. 2008. 内蒙古达茂旗北部早古生代花岗岩类SHRIMP U-Pb年代学[J]. *地质学报*, 82(6): 778 ~ 787.
- 赵利刚, 冉皞, 张庆红, 等. 2012. 内蒙古阿巴嘎旗奥陶纪岩体的发现及地质意义[J]. *世界地质*, 31(3): 451 ~ 461.